Palaeogeography, Palaeoclimatology, Palaeoecology 534 (2019) 109278

Contents lists available at ScienceDirect

Palaeogeography, Palaeoclimatology, Palaeoecology

journal homepage: www.elsevier.com/locate/palaeo

Biogenic silica and organic carbon fluxes provide evidence of enhanced marine productivity in the Upper Ordovician-Lower Silurian of South China

Maliha Zareen Khan[a], Qinglai Feng[a,b,*], Ke Zhang[a], Wei Guo[a]

[a] State Key Laboratory of Geological Processes and Mineral Resources, China University of Geosciences, Wuhan, Hubei 430074, PR China
[b] School of Earth Science, China University of Geosciences, Wuhan, Hubei 430074, PR China

ARTICLE INFO

Keywords:
Radiolarians
Total organic carbon
Wufeng-Longmaxi formations
Redox conditions
Palaeoproductivity proxies

ABSTRACT

Biogenic silica is a powerful palaeoproductivity proxy in palaeomarine environments and is significant within shale gas reservoirs, demonstrating the association of marine hydrocarbon source rocks with the abundance of micro-siliceous fossils, yet detailed studies that investigate this strong alliance in the Ordovician-Silurian transition are still lacking. The bulk of TOC in marine sediments is commonly assumed to have been derived predominantly from marine phytoplankton, with modern ocean surveys indicating good correspondence between silica content and primary productivity. This study discovers a strong positive correlation between biogenic silica (Bio-Si) and TOC in the Upper Ordovician-Lower Silurian Wufeng and Longmaxi formations of South China in the Jiaoye 41-5 ($R = +0.68$, $p(\alpha) < 0.01$, $n = 69$) and Jiaoye 51-2 ($R = +0.68$, $p(\alpha) < 0.01$, $n = 48$) cores, implying that enhanced marine productivity has a strong effect on organic carbon enrichment. Geochemical and palaeontological analyses revealed that silica within these shales generally had a biogenic origin in Jiaoye 41-5 and Jiaoye 51-2, subsequently modified by silica dissolution and re-crystallization of radiolarians and sponge spicules. Palaeoproductivity proxies, including biogenic silica, barium, phosphorous, copper and nickel, were applied, together with the occurrence of pyritized or "ghost" radiolarians, to confirm high palaeoproductivity in the O-S transition. Synchronous OCAR and Bio-SiAR profiles imply that silica originating from siliceous organisms (Bio-Si) served as a likely vector for organic carbon enrichment in the Palaeozoic Wufeng-Longmaxi marine siliceous source rock, providing two possibilities: (i) the abundance of radiolarians was linked to algal proliferation, and consequently, high productivity resulted in a large organic carbon flux and/or (ii) radiolarians contributed to TOC (supported by studies revealing that modern radiolarians exhibit lipid contents of up to 47%).

1. Introduction

Jiaoshiba shale gas field was the first shale gas field in China and has attracted widespread interest. This field has an area of approximately 347 km^2 and is located in Jiaoshiba Town, Fuling District, Chongqing. The Sichuan Basin and its surrounding areas are major targets for shale gas exploration and development in the Wufeng-Longmaxi (also known as Lungmachi) formations. By the end of 2017, the cumulative gas production from the Wufeng and Longmaxi formations at Jiaoshiba exceeded 14 billion cubic metres (Nie et al., 2018). The Wufeng-Longmaxi formations preserve a continuous stratigraphic record of the Upper Ordovician-Lower Silurian black shale sequence on the Upper Yangtze Platform in South China (Chen et al., 2004; Su et al., 2007). However, the mechanism of organic-rich shale deposition in this succession is still under much debate.

Several hypotheses have been proposed, including enhanced preservation due to anoxic conditions (Wang et al., 2008), high palaeoproductivity (Tenger et al., 2006; Zhou et al., 2015), sea-level changes (Liu et al., 2016), restricted basin conditions (Mou et al., 2011), and/or any combination of these factors (Yan et al., 2012; Zeng et al., 2011). Several researchers have suggested an association between marine hydrocarbon source rocks and abundant micro-siliceous fossils (especially radiolarians) and siliceous rocks (Zhang et al., 2007; Li et al., 2009; Xia et al., 2010). Despite existing research, no detailed studies have been undertaken in the Upper Ordovician-Lower Silurian Wufeng and Longmaxi formations to unravel this phenomenon and to determine exactly how silica is related to organic matter enrichment.

The authors intend to study the salient factors affecting organic carbon accumulations during deposition of the Upper Ordovician-Lower Silurian Wufeng and Longmaxi marine shale succession. This

* Corresponding author at: State Key Laboratory of Geological Processes and Mineral Resources, China University of Geosciences, Wuhan, Hubei 430074, PR China.
E-mail address: qinglaifeng@cug.edu.cn (Q. Feng).

https://doi.org/10.1016/j.palaeo.2019.109278
Received 28 September 2018; Received in revised form 19 July 2019; Accepted 19 July 2019
Available online 06 August 2019
0031-0182/

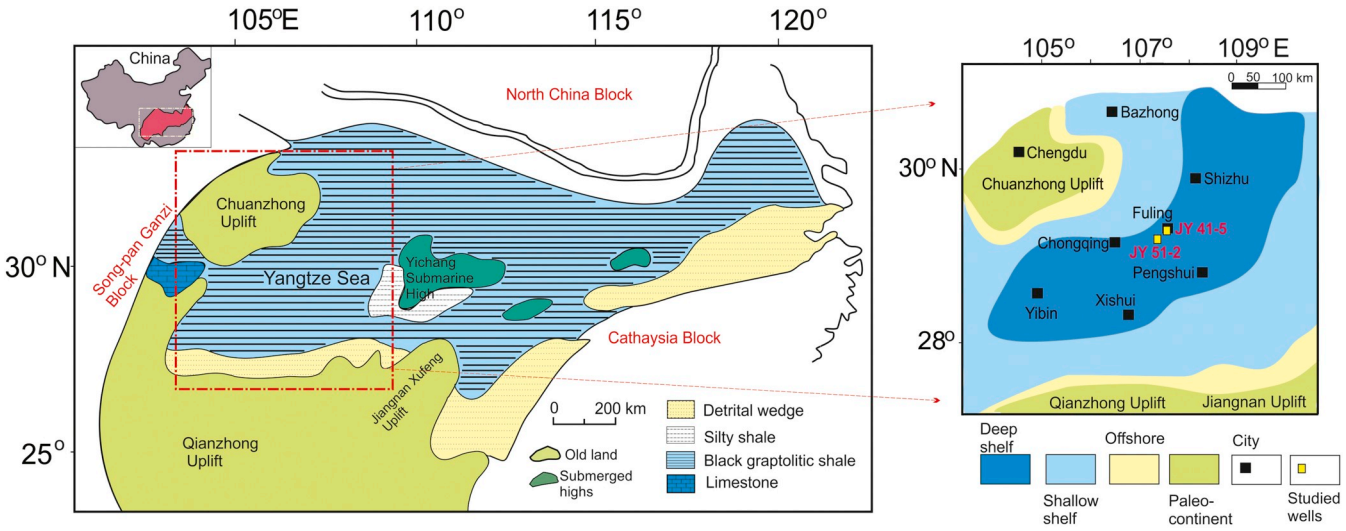

Fig. 1. (Left) Lithofacies palaeogeographic map of the Yangtze block during the Late Ordovician Wufeng interval (modified from Chen et al., 2004) & (right) location of drillcore sections Jiaoye (41-5) and Jiaoye (51-2) (modified from Liang et al., 2009 and Guo, 2013).

research scrutinizes the direct relationship between biogenic silica (Bio-Si) and total organic carbon (TOC) and whether Bio-Si could be a good indicator for organic matter enrichment.

Two drillcore sections were studied (Jiaoye 41-5 and Jiaoye 51-2) composed of the Upper Ordovician-Lower Silurian Wufeng and Longmaxi formations, located in the southeastern area of Chongqing (Fig. 1). This research utilizes geochemical proxies, including Bio-Si, barium, phosphorous, copper, nickel, redox-sensitive trace elements and microfossil palaeontological analysis, as well as a review of Bio-Si occulation and radiolarian contribution to organic matter in modern oceans.

2. Geological setting

The Yangtze Platform was located on the South China Craton, which was a separate plate during the Palaeozoic but still attached to the margins of Gondwana during the Ordovician-Early Silurian transition (Metcalfe, 1994; Shen et al., 2019) and covered by a broad epeiric sea (Yangtze Sea) bordered by the ancient Southeast China Sea (Wang et al., 1997). From the Late Ordovician to Early Silurian, due to the Kwangsian movement (Chen et al., 2014), the Upper Yangtze Platform underwent compression that formed the Chuanzhong Uplift in the northwest, the Qianzhong Uplift in the south and the Jiangnan-Xuefeng Uplift in the southeast, resulting in the evolution of an enclosed basin (Liang et al., 2009). Due to the development of several uplifts, the marine area was reduced to the northeast, east and southeast, with a relative rise in sea level (Wang et al., 1997; Li et al., 2017). Consequently, the Yangtze carbonate platform gradually evolved into a siliciclastic-dominated deep shelf basin (Chen et al., 2006), with relatively low energy and anoxic conditions prevailing in the southeastern Sichuan Basin (Wang et al., 2009; Zhao et al., 2017) (Fig. 1).

Two large global transgressions occurred in the Late Ordovician and Early Silurian, resulting in sedimentary deposition of the Wufeng and Longmaxi formations (Su et al., 2007). The studied area encompasses the Wufeng Formation, Guanyinqiao Member (also known as Kuanyinchiao) and Longmaxi Formation in ascending order. Eight graptolitic biozones and one brachiopod fauna were established from Jiaoye 41-5 (Table 1). Amongst them, two graptolitic biozones belong to the Katian (Upper Ordovician), two graptolitic biozones and one brachiopod fauna are grouped into the Hirnantian, and four graptolitic biozones are assigned to the Llandovery (Lower Silurian; Shen et al., 2019).

The thin, black, graptolitic Wufeng siliceous shale developed due to a prevailing shallow continental shelf and marginal sea environment and has an average thickness of 10 m across the study area. Three graptolitic biozones are recognized in the Wufeng Formation at Jiaoye 41-5, including the *Dicellograptus sichuanensis* Biozone (Chen et al., 2004), *Paraorthograptus pacificus* Biozone (formed by *Tangyagraptus typicus* and *Diceratograptus mirus* Biozones from the lower-middle parts of the Wufeng Formation) and *Metabolograptus extraordinarius* Biozone from the upper part of the Wufeng Formation. Using the first two biozones, the lower to middle parts of the Wufeng Formation are correlated to the Late Ordovician Katian Stage, and the uppermost *Metabolograptus extraordinarius* Biozone should belong to the Late Ordovician Hirnantian Stage (Chen et al., 2006; Gradstein et al., 2012; Chen et al., 2012). The overlying Guanyinqiao Member is a thin horizon of shell-rich marl ~0.5 m thick deposited during a rapidly falling sea level and attributed to the Hirnantian glaciations containing *Hirnantia* fauna (Zhao et al., 2017; Chen et al., 2004, 2006).

The lowermost Longmaxi Formation is composed of black carbonaceous shale deposited due to an increase in sea level and further deepening of the water column (Liang et al., 2009; Guo, 2013) in a deep sea-shelf basin (Zeng et al., 2011). Subsequently, the development of uplifts and an increase in sediment supply led to an upward coarsening of the succession. Consequently, in the Longmaxi Formation, five biozones have been recognized in ascending order: *Metabolograptus persculptus* Biozone, *Parakidograptus acuminatus* Biozone, *Orthograptus vesiculosus* Biozone, *Pristiograptus leei* Biozone and *Demistrites triangulates* Biozone. Of these biozones, the first biozone belongs to the Hirnantian, three to the Rhuddanian and one to the Aeronian stages (Piccara et al., 1995; Storch and Kraft, 2009; Chen et al., 2006; Gradstein et al., 2012; Chen et al., 2015). It should be noted that the index fossils of the first graptolitic biozone from the Silurian, namely, *Akidograptus ascensus* Biozone (Gibbons and Morena, 2002; Gradstein et al., 2012; Table 1), are absent in this study. Therefore, the Ordovician-Silurian boundary (OSB) is correlated at the base of the *Parakidograptus acuminatus* Biozone (Table 1, Fig. 3).

3. Materials, methodology and calculations

Samples were collected from the two studied sections (Fig. 1) for investigation of geochemical parameters and siliceous microfossils.

Sixty-nine samples were collected from Jiaoye 41-5 (29.628°N, 107.541°E), incorporating seventeen samples from the Wufeng Formation (including two from the Guanyinqiao Member) and 52 from the Longmaxi Formation. Forty-eight samples were collected from

Table 1
Subdivision of the Ordovician-Silurian graptolite biozones in the Yangtze region (Gradstein et al., 2012; Chen et al., 2012; Chen et al., 2015; Shen et al., 2019) through the Ordovician and Silurian transition.

Series	Stage	Formation	Depth	Graptolite Biozones		Age (Ma)
Early Silurian	Aeronian	Longmaxi	2570.4–2577.24 m LM_6	*Demistrites triangulates*		440.77
	Rhuddanian		2577.24–2599.99 m LM_5	*Pristiograptus leei-petalolithus*		441.57
			2599.99–2612.15 m LM_4	*Orthograptus vesiculosus*		442.47
			2612.15–2612.9 m LM_{2-3}	*Parakidograptus acuminatus* *Akidograptus ascensus?*		443.40
	Hirnantian		2612.9–2613.28 m LM_1	*Metabolograptus persculptus*		444.43
		GYQ	2613.28–2613.41 m	*Hirnantia*		
			2613.41–2614 m WF_4	*Metabolograptus extraordinarius*		445.16
Late Ordovician	Katian	Wufeng	2614.0–2614.87 m WF_3	*Paraorthograptus pacificus*	*Dicera-tograptus mirus* *Tangyagraptus typicus* *Lower subzone*	447.02
			2614.87–2617.74 m WF_2	*Dicellograptus sichuanesis*		447.62

Jiaoye 51-2 (29.613°N, 107.588°E), comprising six samples from the Wufeng Formation (including one from the Guanyinqiao Member) and 42 from the Longmaxi Formation. Previous works focused on the mercury cycle of these two sections (Shen et al., 2019), whereas this study concentrates on palaeoproductivity variations.

3.1. Analytical procedures

Quantitative analysis of radiolarian tests and sponge spicules was conducted at the State Key Laboratory of Geobiology and Environmental Geology, with scanning electron microscopy (SEM) performed at the State Key Laboratory of Geological Processes and Mineral Resources, China University of Geosciences (Wuhan).

Each sample (150 g) was crushed to approximately 2 cm detritus, placed in dilute (3%) hydrofluoric acid (HF) for eight hours and then rinsed. After repetition of this process until all samples had disintegrated, the residues were sieved (0.054 mm mesh) and dried. The radiolarian tests and sponge spicules were quantified using an optical microscope (Olympus SZ51), and well-preserved specimens were picked from the dry residue for taxonomic identification. Specimens were counted as an individual where the shell was at least three-quarters preserved or where two large or three small fragments were found. The best preserved specimens were mounted on stubs and photographed using a FEI SEM Quanta 200 scanning electron microscope for more precise determinations. To supplement this analysis, 20 thin sections from Jiaoye 51-2 were studied under optical microscopy (Leica STP 6000), for which slides were prepared from > 45 μm fractions using standard techniques (Lazarus, 1994).

Fresh samples for geochemical investigations were pulverized to 0–200 mesh in an agate mortar. Major element concentrations were analysed at the State Key Laboratory of Geological Processes and Mineral Resources at China University of Geosciences (Wuhan). Oxides were determined by chemical titration methods. Taking SiO_2 as an example, powdered samples were fused with the fluxing agent Na_2CO_3, leached with HCl, evaporated to a small volume of coacervate silicate with polyethylene oxide, filtered, and heated, and then the solid was weighed as M1. SiO_2 was extracted as SiF_4 through dissolution in hot HF and H_2SO_4, and the remaining solid was weighed as M2. Residues were fused again with fluxing agent $K_2S_2O_7$ and extracted using distilled water. The solution was combined with the previous HCl filtrate, and after depolymerization, residual SiO_2 in the filtrate was measured as M3 using molybdenum blue spectrophotometry. Finally, the total SiO_2 concentration was calculated as (M1 − M2 + M3). The results show an accuracy of ± 0.1% for reported SiO_2 contents based on replicate analysis of Chinese national standard GB/T 14506.3-2010 (Yuan et al., 2016). The oxide concentrations of Al, Fe, Ca, Mg, P, Mn, K and Na were determined by similar methods with a corresponding degree of accuracy (± 0.1%) based on Chinese national standard GB/T 14506 (Liu et al., 2018).

Trace elements were determined by an Agilent 7500a inductively coupled plasma mass spectrometer (ICP-MS) at the State Key Laboratory of Geological Processes and Mineral Resources, China University of Geosciences (Wuhan), with an analytical precision better than 5%. TOC was measured using a Jena multi-EA 4000 carbon-sulphur analyser through online combustion at 1350 °C after samples were fully digested in 6 mol/L HCl and rinsed with ultrapure water. Analytical errors were < ± 0.2% for TOC based on replicate analysis of Alpha Resources standard AR 4007.

3.2. Origin of siliceous rocks

Many investigations show that siliceous sediments in marine environments originate mainly from terrigenous, biogenic and hydrothermal origins (Dapples, 1967; Yamamoto, 1987; Rona, 1988). Siliceous rocks deposited by biological and hydrothermal sedimentation are common, with those originating from biogenic sources generally having low contents of Al_2O_3, TiO_2, FeO and MgO. This research utilizes three comparative methods of verification to confirm the origin of siliceous rocks:

(i) The Al-Fe-Mn ternary diagram provides a simple method to characterize the depositional environments of shales (Adachi et al., 1986; Yamamoto, 1987; Shi et al., 2016).

(ii) The ratio (Al/Fe + Al + Mn) indicates the relative contribution of continental versus oceanic detritus or whether a large submarine exhalative contribution existed (Boström et al., 1973).

(iii) The Si/(Si + Fe + Al + Ca) ratio provides information on the Bio-Si content in relation to alumino-silicates and ferruginous and calcareous minerals (Rangin et al., 1981; Ruiz-Ortiz et al., 1989; Ran et al., 2015; Zhao et al., 2017).

3.3. Geochemical proxies

Bio-Si is a powerful proxy in marine sediments and an important indicator for studying siliceous organism distribution and palaeoproductivity. Since silica is a key marine nutrient, local primary productivity and palaeo-upwelling activities can be inferred by analysing Bio-Si deposited in sediments (Chou et al., 2012). The significantly higher Si content of organic-rich shales than of organic-poor shales

Table 2
Statistics of sedimentation rate of the Wufeng-Longmaxi formations in Jiaoye 41-5 (left) and Jiaoye 51-2 (right).

Jiaoye 41-5				Jiaoye 51-2					
Graptolite biozone	Thickness (m)	Duration (Ma)	LSR (m.Ma^{-1})	Stage	Formations	Graptolite biozone	Thickness (m)	Duration (Ma)	LSR (m.Ma^{-1})
439.21 *Demistrites triangulatus* 440.77	19.7	1.56	12.63	Aeronian	Longmaxi				
Pristiograptus leei-petalolithus 441.57	22.26	0.8	28.32	Rhuddanian		*Pristiograptus leei-petalolithus*	19.77	0.8	24.71
Orthograptus vesiculosus 442.47	12.25	0.9	13.61			*Orthograptus vesiculosus*	14.14	0.9	15.71
Parakidograptus accuminatus 443.40 443.83?	0.75	1.36	0.55			*Parakidograptus accuminatus*	3.9	1.36	2.87
Metabolograptus persculptus 444.43	0.38	0.6	0.63	Hirnantian		*Metabolograptus persculptus*	3.1	0.6	5.17
Hirnantia *Metabolograptus extraordinarius* 445.16	0.13 0.59 0.72	0.73	0.99		GYQ Wufeng	*Hirnantia* *Metabolograptus extraordinarius*	1.5	0.73	2.05
Paraorthograptus pacificus 447.02	0.87	1.86	0.46	Katian		*Paraorthograptus pacificus*	2.8	1.86	1.51
Dicellograptus sichuanesis 447.62	2.87	0.60	4.78						

indicates the existence of Bio-Si (Chalmers et al., 2012; Shen et al., 2012; Xiang et al., 2013). Siliceous organisms, including radiolarians and other plankton with siliceous skeletons, extract dissolved silica from the surface layer of oceanic water to form their tests. Consequently, Bio-Si levels can indicate changes in productivity in time and space (Lyle et al., 1988).

In palaeomarine environments, Bio-Si equals the total silica in every sample deducting its terrigenous input and can therefore be calculated as follows (Ross and Bustin, 2009; Shen et al., 2012; Xiang et al., 2013; Arsairai et al., 2016):

$$\text{Excess } SiO_2\ (\%) = SiO_{2\,(\text{sample})} - Al_{(\text{sample})} \times (SiO_2/Al)_{PAAS} \quad (1)$$

Excess SiO_2 represents Bio-Si, and $SiO_{2\,(\text{sample})}$ and $Al_{(\text{sample})}$ are the tested concentrations of SiO_2 and Al in each sample. $(SiO_2/Al)_{PAAS}$ represents the ratio of SiO_2/Al in Post-Archean Australian Shale (Taylor and McLennan, 1985). Linear sedimentation rates (LSR) were calculated for identified graptolitic biozonations in the Wufeng and Longmaxi formations (see Table 2) as follows:

$$\text{LSR} = \text{thickness/duration} \quad (2)$$

To assess variations in palaeoproductivity (Figs. 3 and 4), the mass accumulation rates (MAR) of TOC and Bio-Si were calculated as follows:

$$(X)\ \text{AR} = \text{Concentration}\ (X) \times \text{LSR} \times \rho \quad (3)$$

where X is the proxy of interest (TOC or Bio-Si), LSR is linear sedimentation rate (m Myr^{-1}) and ρ is sample bulk density, which, for convenience, was assumed to be 2.5 g cm^{-3} for all samples (Algeo et al., 2013; Shen et al., 2015; Wang et al., 2019). The MAR of TOC and Bio-Si are abbreviated as OCAR and Bio-SiAR, respectively, with units of g m^{-2} yr^{-1} (Figs. 3 and 4). Note that LSR multiplied by ρ is equal to the sediment bulk accumulation rate (BAR).

Copper and nickel, to a large extent, are fixed with pyrite in sulphidic marine sediments and serve as markers for relatively high organic matter flux (Tribovillard et al., 2006; Ingri et al., 2014). Cu is an essential micronutrient for phytoplankton, which are part of the biogeochemical cycle (Sunda et al., 1981). Primary producers absorb Cu during photosynthesis to form organic matter that can be preserved in sediments upon decomposition (Piper and Perkins, 2004; Tribovillard et al., 2006; Shen et al., 2014). The high tendency of copper to complex with organic matter suggests that it could be used as a palaeoproductivity proxy, specifically in reducing environments where it forms stable sulphides (Shen et al., 2014).

Nickel is involved in the biogeochemical cycle and deep regeneration characteristics of all chemical species incorporated in organisms. Nickel regenerates as silicates in deep waters instead of forming phosphates as at shallow depths (Sclater et al., 1976). Ni occurs in highly stable tetrapyrrole complexes originally derived from chlorophyll that are preferentially preserved under anoxic conditions (Lewan and Maynard, 1982). Where organic matter has been extensively exposed to aerobic conditions, the preservation of these complexes is poor, and the subsequent organic matter has a low Ni content (Porter et al., 2014). Under extreme reducing conditions, Ni may be incorporated into pyrite as insoluble NiS (Huerta-Diaz and Morse, 1992; Morse and Luther III, 1999); hence, Ni could be a reliable palaeoproductivity proxy.

Van der Weijden (2002) suggested that aluminium normalization of elemental concentrations is a useful procedure for examining the degree of enrichment of an element in sediments. Aluminium can be considered an indicator for aluminosilicate fractions of sediments, having very little ability to move during diagenesis in most sedimentary deposits (Calvert and Pedersen, 1993; Piper and Perkins, 2004; Tribovillard et al., 2006; Reolid et al., 2012).

Barite, which forms during decomposition of plankton (Griffith and Paytan, 2012), is assumed to be the major carrier mineral of barium from seawater to sediments. In marine sediments, Ba is also abundant in biogeochemical phases such as carbonates, organic matter and Bio-Si (Robin et al., 2003). Normalized Ba/Al is extensively utilized as a proxy for palaeoproductivity (Reolid et al., 2012; Shen et al., 2015). The relationship between barite and organic carbon flux in ocean sediment traps has been used as a potential indicator for primary productivity (Dymond et al., 1992). Authigenic barite can dissolve under conditions of bacterial sulphate reduction, whereas it is enriched under oxic conditions (Bishop, 1988; Dehairs et al., 1991; Dymond et al., 1992).

Phosphorus is an essential nutrient for marine phytoplankton growth and is a structural and functional component of all organisms (Redfield, 1960). Organic matter is the ultimate source of most phosphorus in marine sediments (Ingall et al., 1993) owing to its close association with organic carbon and can be deposited in sediments associated with the remains of organisms (Schenau et al., 2005; Schoepfer et al., 2015). However, in permanently anoxic environments with sulphidic bottom waters, due to potential adsorption and complexed remineralization, organic P is reduced (Tribovillard et al., 2006). P accumulation rates have been used as productivity indicators in both modern and ancient sediments (Schenau et al., 2005).

Uranium (authigenic) enrichment in sediments is controlled by the oxygen penetration depth and sedimentation rate (Tribovillard et al., 2006; Arsairai et al., 2016). Thorium is relatively immobile in low-temperature surface environments and concentrates during weathering in resistant minerals. Therefore, high U/Th values may indicate high organic matter accumulation, as U also tends to be enriched in marine sediments under reducing conditions (Algeo and Maynard, 2004; Tribovillard et al., 2006). Consequently, U/Th ratios can reflect redox conditions during deposition. In general, a ratio of U/Th > 1.25 indicates an anoxic environment, 0.75–1.25 indicates a dysoxic environment and U/Th < 0.75 indicates an oxidizing environment (Wignall and Myers, 1988).

4. Results

4.1. Silica source determination

The Al-Fe-Mn ternary diagram (Fig. 2) shows that most shale samples from Jiaoye 41-5 have low Mn concentrations, with most siliceous rocks located in the non-hydrothermal area (i.e., biogenic origin). Likewise, samples from Jiaoye 51-2 illustrate that a biogenic origin is dominant in the studied section. Both Jiaoye 41-5 and 51-2 demonstrate extremely low values of Mn.

The ratio of Al/(Fe + Al + Mn) ranges from 0.4 to 0.8 for Jiaoye 41-5 (average 0.7) and 0.5–0.7 for Jiaoye 51-2 (average 0.7). The average values for radiolarite beds are generally lower than 0.6, which is considered the mean for biogenic hemipelagic chert (Adachi et al., 1986).

All samples from the Wufeng and Longmaxi formations present Si/(Si + Fe + Al + Ca) values ranging from 0.4 to 0.9 in Jiaoye 41-5 (average 0.7) and 0.4 to 0.8 in Jiaoye 51-2 (average 0.7). Al is considered the principal proxy for clay mineral flux in fine-grained clastic deposits, whereas Si is mainly present in both siliciclastic and biogenic fractions. Typical silica-rich radiolarite beds have values of 0.8–0.9 (Ruiz-Ortiz et al., 1989).

4.2. Geochemical results

Five distinct stages were recognized on the basis of enrichment and preservation of organic matter in both Jiaoye 41-5 and Jiaoye 51-2: Stages I–III (Wufeng Formation) and Stages IV–V (Longmaxi Formation), as illustrated in Figs. 3 and 4.

4.2.1. Jiaoye 41-5

Stage I (well depth from 2619.36 to 2618.8 m) positioned in the lower part of the *Dicellograptus sichuanensis* Biozone shows low productivity values and TOC ranging from 0.2% to 0.8%. Ba/Al ranges from 194 to 217 with Bio-Si values of 0% to 7.1%. The U/Th ratios of 0.11–0.16 indicate that the oxic environment progressively evolved into an oxygen-poor and even hypoxic environment. Cu and Ni display a similar pattern, with values of 94–148 ppm and 44–51 ppm, respectively (Fig. 3). Ba/Al and P/Al values exhibit increasing productivity. OCAR and Bio-SiAR exhibit low values in Stages I and III. Stage II (well depth from 2618.80 to 2613.41 m) from the *Dicellograptus sichuanensis* to *Metabolograptus extraordinarius* Biozones shows a high productivity period with all geochemical indicators displaying high values. This organic-rich stage displays U/Th ratios of 0.27–2.20 (average of 1.46) with most values > 1.25, suggesting an anoxic environment mainly characterized by hypoxia. TOC shows a high value of 6.2%; Bio-Si, 67.4%; Cu, 136 ppm; and Ni, 405 ppm. Ba/Al and P/Al increase upwards following TOC, and OCAR and Bio-SiAR show high values with maximums of 67.2 g m^{-2} yr^{-1} and 785 g m^{-2} yr^{-1}, respectively. Stage III (well depth from 2613.41 to 2613.28 m) from the end of the *Metabolograptus extraordinarius* to the beginning of the *Metabolograptus persculptus* Biozones demonstrates the OSB at the Guanyinqiao Member. Organic matter shows an abrupt decline with low palaeoproductivity indicators exhibiting a decrease in productivity in this stage compared to that in Stage II. This stage of the OSB yields U/Th values of 0.36–1.20, suggesting an abrupt shift from sub-oxic to oxic environments.

Stage IV (well depth from 2613.28 to 2585.15 m) from the *Metabolograptus persculptus* to *Pristiograptus leei* Biozones was possibly a recovery stage for producers from the Hirnantian Stage. TOC ranges from 2.3% to 7.0%, and Bio-Si exhibits values of 13.0% to 50.9%. U/Th ratios of 0.58–4.30 suggest a sub-oxic to anoxic environment. Cu ranges from 33 ppm to 82 ppm, and Ni displays values of 72 ppm to 128 ppm.

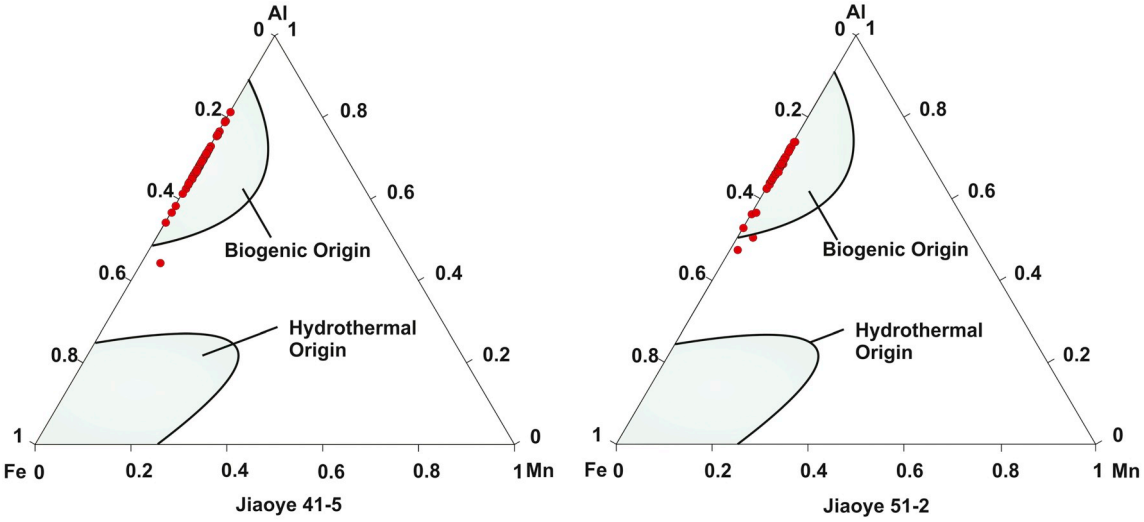

Fig. 2. Al-Fe-Mn diagram for Jiaoye 41-5 and Jiaoye 51-2.

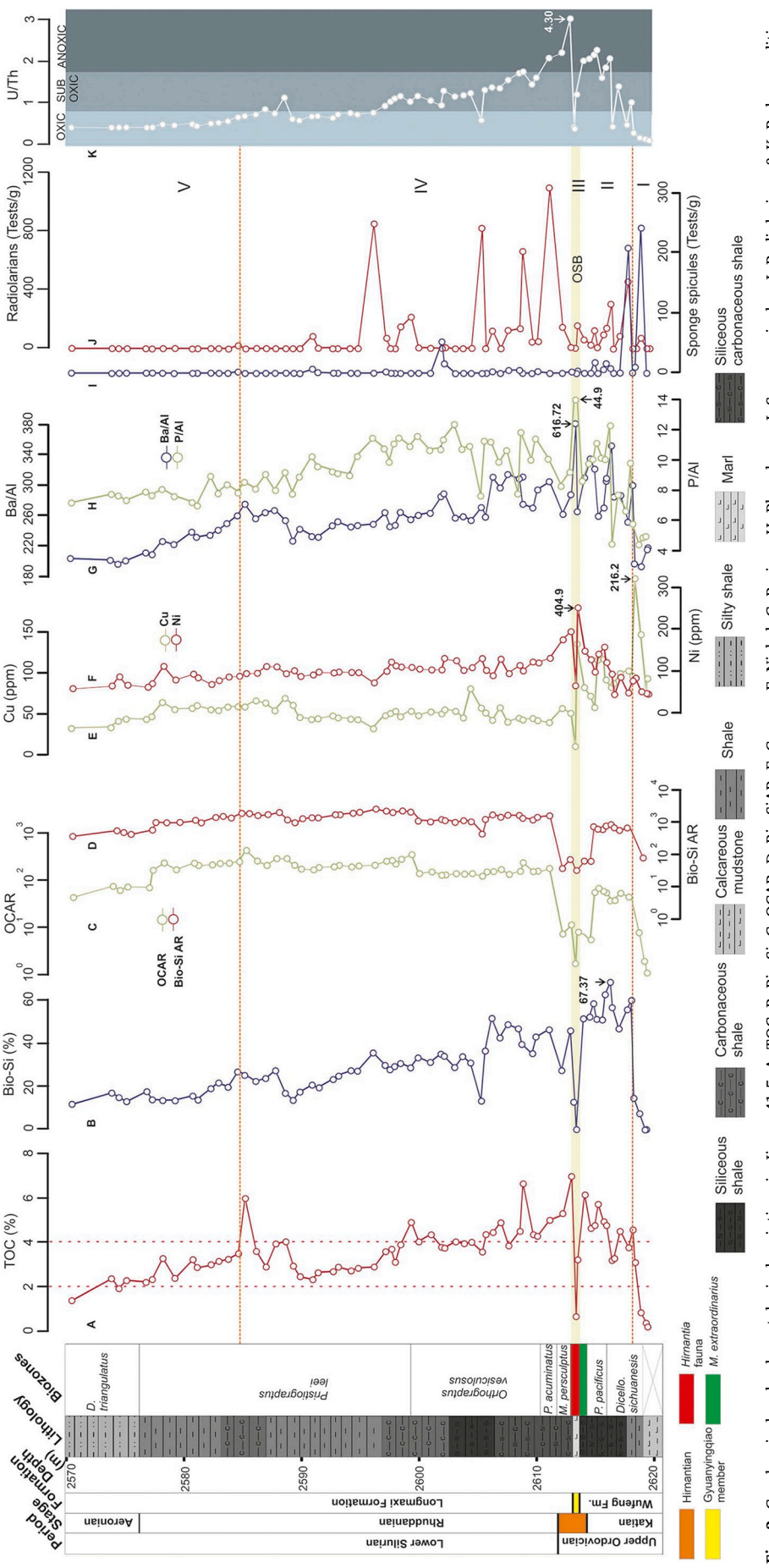

Fig. 3. Geochemical and palaeontological variations in Jiaoye 41-5. A: TOC, B: Bio-Si, C: OCAR, D: Bio-SiAR, E: Copper, F: Nickel, G: Barium, H: Phosphorus, I: Sponge spicules, J: Radiolarians, & K: Redox conditions proxy; U/Th.

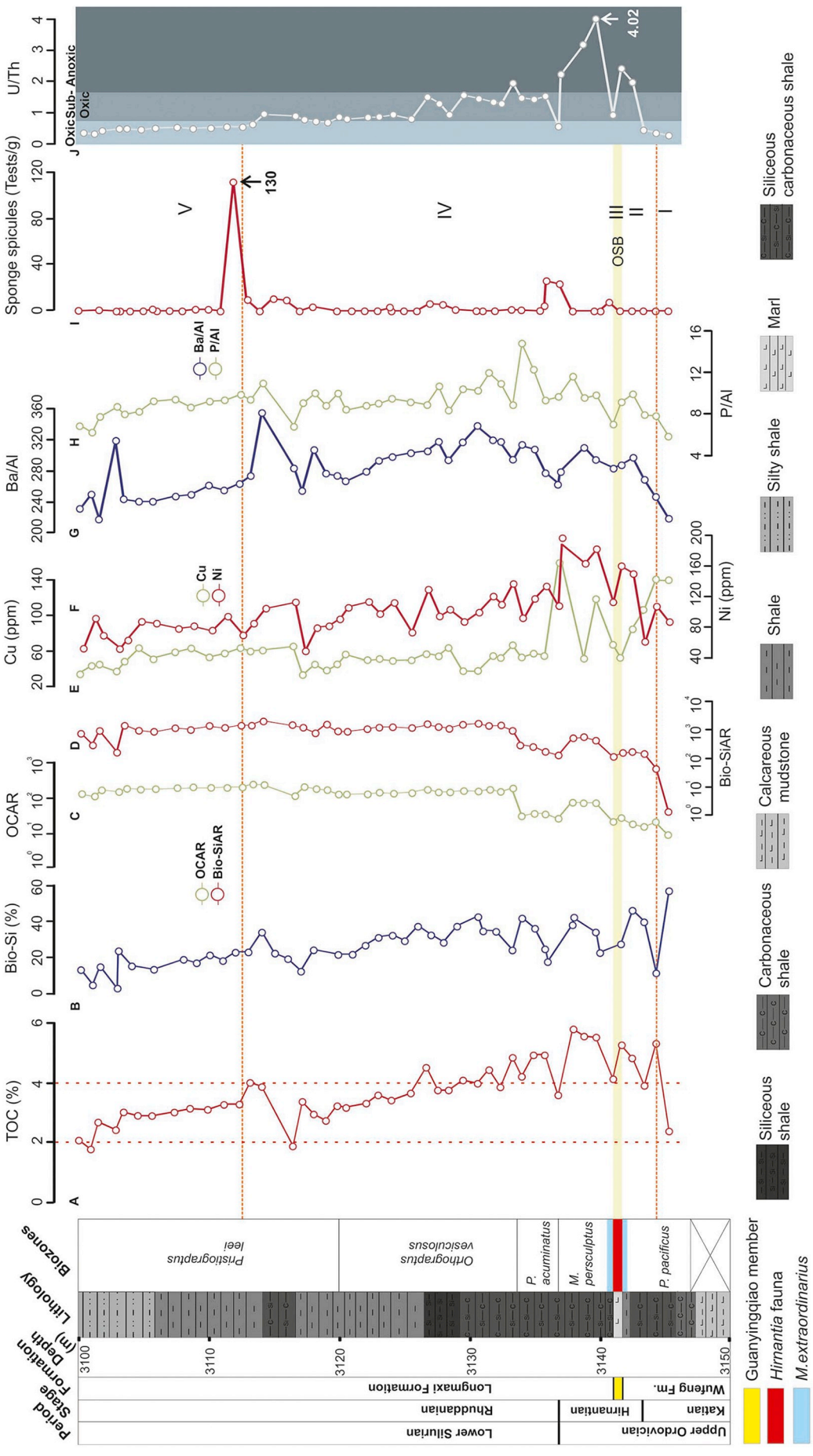

Fig. 4. Geochemical and palaeontological variations in Jiaoye 51-4. A: TOC, B: Bio-Si, C: OCAR, D: Bio-SiAR, E: Copper, F: Nickel, G: Barium, H: Phosphorus, I: Sponges & J: Redox conditions proxy; U/Th.

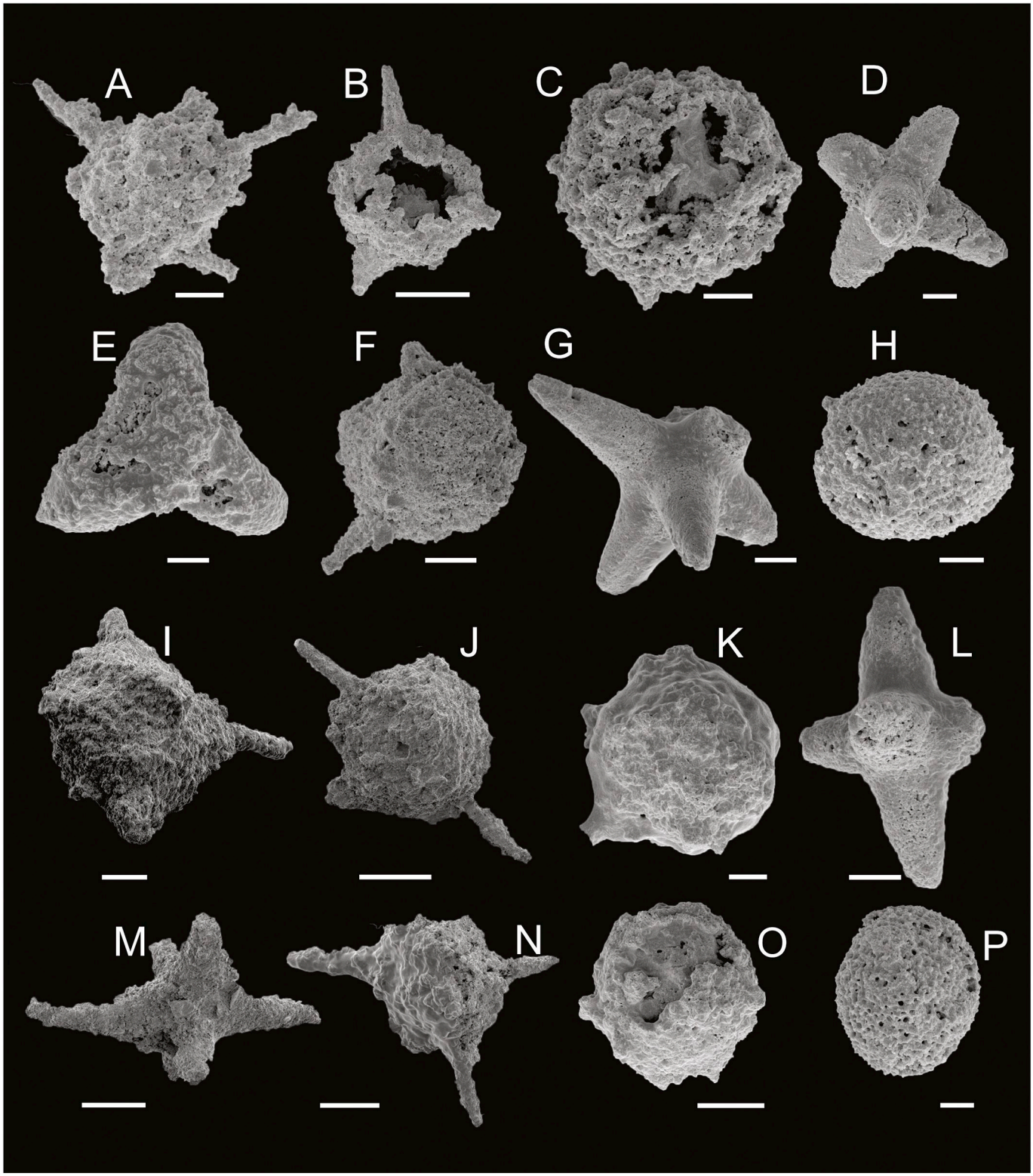

Fig. 5(A). Radiolarians and sponge spicules from Jiaoye 41-5. A, B, C, F, H, I, J, N, P: Radiolaria gen. et sp., Indet. D, G, L, M: Hexactines, E: Triactine, O, K: Syntagentactinia.

Ba/Al and P/Al concisely follow the pattern of TOC accumulation (Fig. 3). OCAR and Bio-SiAR start to increase from the *Parakidograptus acuminatus* Biozone and then show steady rates until the end of the *Pristiograptus leei* Biozone, with average values of 192 $g\,m^{-2}\,yr^{-1}$ and 1460 $g\,m^{-2}\,yr^{-1}$, respectively. Stage V (well depth from 2585.15 to 2570.40 m) encompasses the upper part of the *Pristiograptus leei* to *Demirastrites triangulatus* Biozones and displays U/Th ratios of 0.39–0.65, indicating a change from sub-oxic to oxic conditions. OCAR and Bio-SiAR display steady rates in the upper Longmaxi Formation at the beginning of the *Demistrites triangulatus* Biozone with minimum values of 42.9 $g\,m^{-2}\,yr^{-1}$ and 358 $g\,m^{-2}\,yr^{-1}$, respectively. Subsequently, this stage yields lower values for all other proxies: 1.4% to

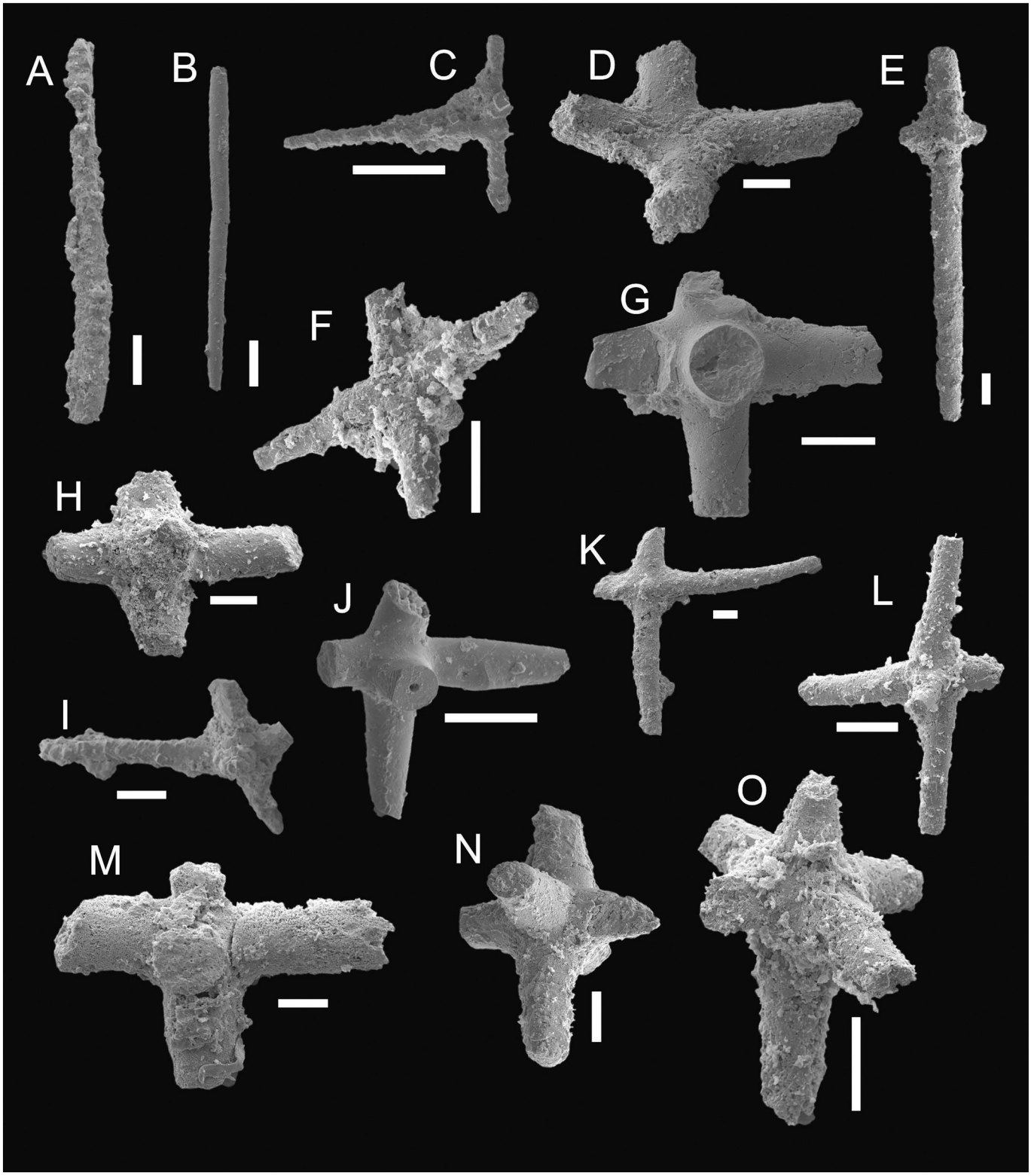

Fig. 5(B). Sponge spicules from Jiaoye 51-2. A–B: Oxeas, C–F: Calthrops, G–O: Orthohexactines.

3.5% for TOC, 11.3%–21.3% for Bio-Si, 33 ppm to 65 ppm for Cu, 57 ppm to 111 ppm for Ni, and ratios of 196 to 260 for Ba/Al and 7.1 to 8.9 for P/Al.

4.2.2. Jiaoye 51-2

Jiaoye 51–2 also exhibits five distinct stages with respect to TOC accumulation. Stage I (well depth from 3145.3 to 3143.4 m) located in the lower to middle Wufeng Formation shows a sudden increase in TOC and Bio-Si values from 2.3% to 5.3% and 0.4% to 40.2%, respectively, with a slight shift in productivity (Fig. 4). Cu and Ni exhibit high values of 140 ppm and 108 ppm, with Ba/Al and P/Al increasing upwards. Redox conditions exhibit an oxic environment with U/Th ratios of 0.26–0.44, along with a gradual increase in TOC and Bio-Si towards the upper part. The OCAR and Bio-SiAR values also increase upwards,

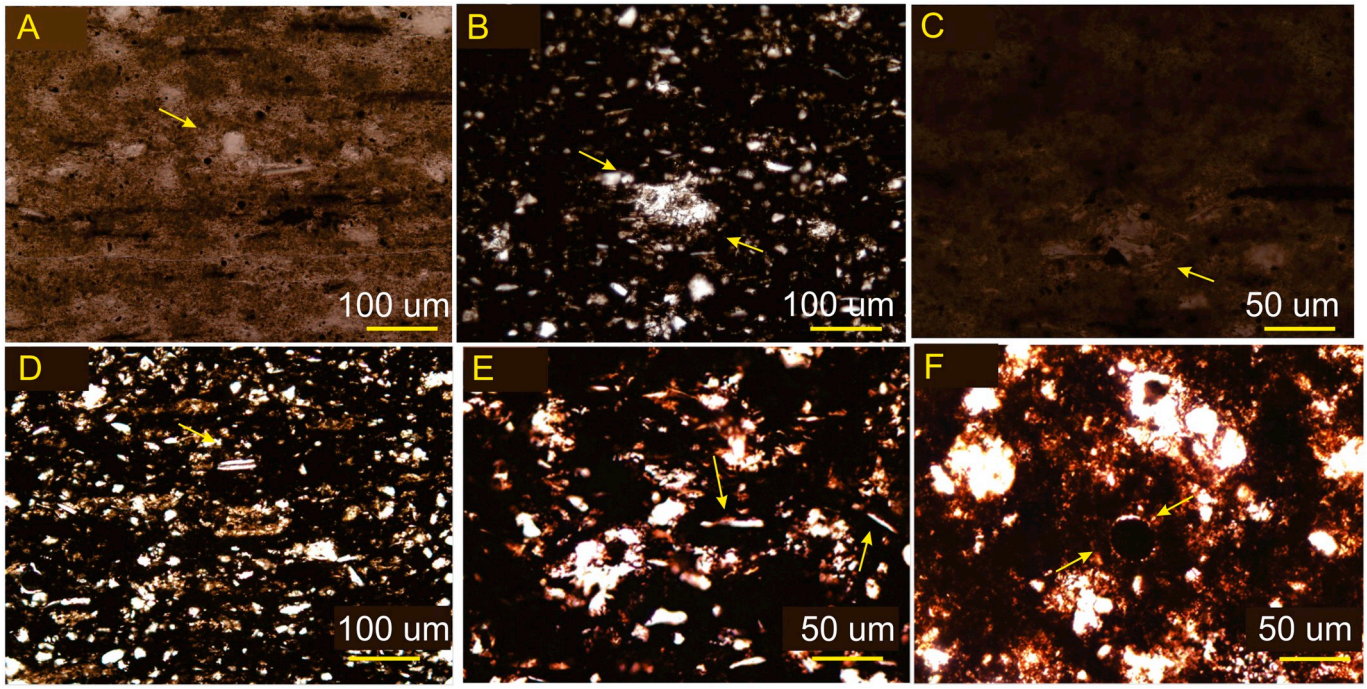

Fig. 5(C). Thin sections of siliceous shale from Jiaoye 41-5 and Jiaoye 51-2. (A–B) Pyritized radiolarian and fossil fragment (yellow arrow); (C) Ghost radiolarian; and (D) Sponge spicules. (For interpretation of the references to colour in this figure legend, the reader is referred to the web version of this article.)

displaying maximum values of 20.1 $g\,m^{-2}\,yr^{-1}$ and 152 $g\,m^{-2}\,yr^{-1}$, respectively. Stage II (well depth from 3143.4 to 3141.6 m) exhibits an increase in productivity coinciding with the *Dicellograptus sichuanensis* to *Metabolograpus extraordinarius* Biozones in Jiaoye 41-5. Along with the Ba/Al (297) and P/Al ratios (9.9), other palaeoproductivity indicators display increasing values from 40.2% to 46.4% and 60 ppm to 150 ppm for Bio-Si and Ni, respectively, with TOC ranging from 4.8%–5.3%. Cu is the exception, showing decreasing values upwards. This stage exhibits U/Th values of 0.91–2.42, indicating the dominance of an anoxic environment. The OCAR values exhibit a slight decrease from Stage I, but the Bio-SiAR values increase, showing a maximum value of 175 $g\,m^{-2}\,yr^{-1}$. Stage III (well depth from 3141.6 to 3139.7 m) from the *Metabolograptus extraordinarius* to the beginning of the *Metabolograpus persculptus* Biozones forms the OSB, resulting in a sudden decrease in productivity and TOC values at the Guanyinqiao Member. All productivity indicators show lower values than those in Stages II and IV, with the exception of U/Th, which shows the highest value of 4.0 in the entire section. The palaeoenvironment shows a change from sub-oxic to anoxic, with accumulation rates for organic carbon and Bio-Si also exhibiting lower values.

Stage IV (well depth from 3139.7 to 3113.2 m) situated between the *Metabolograpus persculptus* and *Pristiograptus leei* Biozones shows high values of TOC, reaching 5.5% in the lower part and decreasing to 3.4% in the middle part of the Longmaxi Formation, with Bio-Si ranging from 12.7 to 42.2%. Ba/Al and P/Al follow a consistent pattern with TOC, whilst Cu and Ni decrease upwards, showing the lowest values of 33 ppm and 49 ppm, respectively. This stage indicates a sub-oxic to anoxic environment with U/Th ratios of 0.53–3.17, with an average of 1.16. OCAR exhibits higher values at the beginning of Stage IV (highest value of 246 $g\,m^{-2}\,yr^{-1}$) but suddenly decreases at the beginning of the *Parakidograptus acuminatus* Biozone, whilst Bio-SiAR mimics the OCAR pattern throughout the stage with values ranging from 129 $g\,m^{-2}\,yr^{-1}$ to 2126 $g\,m^{-2}\,yr^{-1}$ (Fig. 4). Stage V (well depth from 3113.2 to 3095 m) in the upper part of the Longmaxi Formation is related to the *Pristiograptus leei* Biozone, displaying stable values of TOC between 1.8%–3.9% and an average Bio-Si value of 16.0%. This stage indicates an oxic environment with an average U/Th ratio of 0.46, slightly decreasing upwards following the oxic to sub-oxic palaeoenvironmental boundary. Cu ranges between 32 ppm to 64 ppm and Ni from 53 ppm to 95 ppm. In contrast, Ba/Al shows high values against other palaeoproductivity indicators in the section, i.e., TOC, Bio-Si, Cu, Ni and P/Al. OCAR exhibits steady rates, but Bio-SiAR decreases upwards from the middle of Stage V, with a low of 174 $g\,m^{-2}\,yr^{-1}$.

4.3. Siliceous microfossil quantification

Jiaoye 41-5 shows a high concentration of fossils, mainly sponge spicules and solitary radiolarians, with shape types reflecting the lower degree of differentiation (Fig. 5A). Specimen counts were carried out using optical microscopy, and the results are shown in Fig. 3. Stage I yielded good numbers of siliceous sponges (average 81 individuals/g) but showed a low abundance of radiolarians (average 24 individuals/g). Stage II showed sharply increased numbers of well-preserved radiolarians (average 107 individuals/g) but much lower numbers of sponge spicules (average 37 individuals/g). No radiolarian or sponge spicules were recovered from Stage III, whereas Stage IV yielded abundant radiolarians (average 121 individuals/g) but very low numbers of sponge spicules (average 3 individuals/g). Stage V displayed extremely low numbers of well-preserved radiolarians (average 2 individuals/g) with no sponge spicules. Due to poor preservation conditions, the vast majority of individuals cannot be identified. Of those identified, eight were morphological spicule genera and one radiolarian genus (Fig. 5A).

In Jiaoye 51-2 (Fig. 4), no radiolarians were found. Stages I, II and III exhibit no well-preserved sponge spicules, whilst Stages IV and V yielded small amounts of well-preserved sponge spicules (average 4 and 10 individuals/g, respectively) (Fig. 5B). Quantification of radiolarians and sponge spicules did not yield the expected abundance; a plausible reason is that post-depositional diagenesis led to the occurrence of pyritized or “ghost” radiolarians (Fig. 5C).

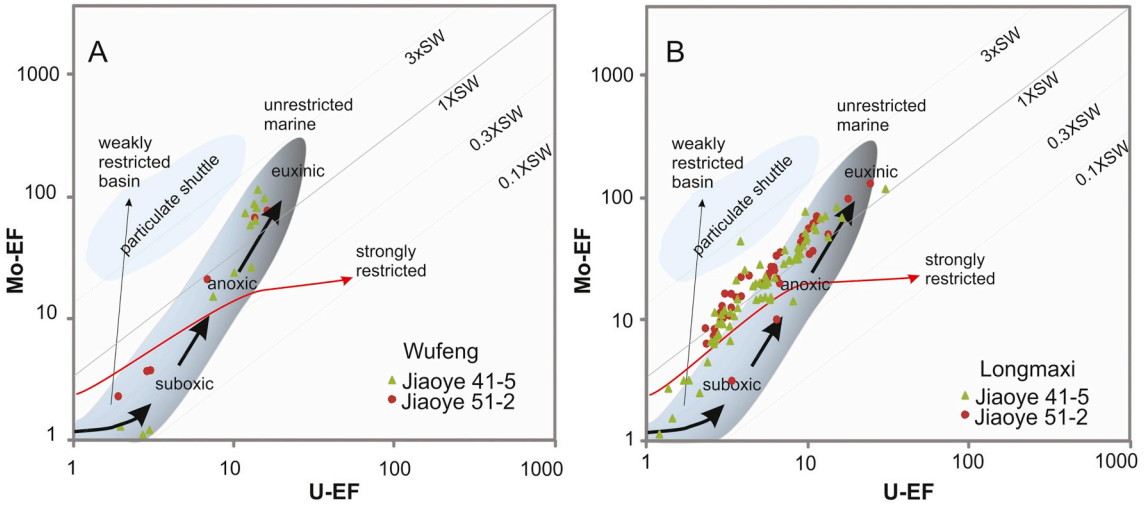

Fig. 6. Enrichment factors (EF) of Mo vs. U, showing that most Wufeng Formation samples plot in areas near the restricted marine euxinic end, whilst most Longmaxi siliceous shale samples plot near the unrestricted anoxic to euxinic end with some at the sub-oxic end (modified from Algeo and Tribovillard, 2009).

5. Discussion

The concentration of organic carbon in marine deposits is controlled by the interplay between the processes of supply and preservation of various components in any given deposit (Calvert and Pedersen, 1993). The input of organic matter, as well as its biological alteration and preservation in marine sediments, is a fundamental biogeochemical process controlled by many factors (Algeo et al., 2016). Generally, it is acknowledged that the most common factors controlling organic matter accumulation and preservation include anoxic conditions during deposition (Wang et al., 2008), high primary productivity (Pedersen and Calvert, 1990; Tenger et al., 2006; Zhou et al., 2015), and clastic input, which controls the dilution of organic-rich sediments (Murphy et al., 2000; Sageman et al., 2003). However, another important controlling factor in marine environments for TOC accumulation and preservation is mineral participation (Weiler and Mills, 1965; Suess, 1973; Muller and Suess, 1977). Analysis of bulk sediments from the coast of Mexico and hydrodynamic fractions from the Peruvian upwelling region suggests that the preserved organic matter is intimately associated with minerals (Hedges, 1995). A variety of nonphyllosilicate clay-sized minerals are often associated with elevated organic matter concentrations, and even amorphous silica (a relatively nonsorptive solid phase) can protect organic matter (Estermann et al., 1959).

The type of association between organic matter and minerals varies in response to organic molecular moiety, size and shape, as well as mineralogy and surface characteristics. Attachments vary along a continuum of mechanisms, from simple adsorption onto mineral surfaces to more physical incorporation into matrices of minerals (Keil and Mayer, 2014). For example, occlusion within mineral grains produced through biotic or abiotic mechanisms and aggregation of colloidal to particulate-sized organic materials with biogenic minerals derived from marine phytoplankton and zooplankton at various levels of complexity (Keil et al., 1997). The strong relationship between very fine-grained minerals and organic matter in sediments leads to the question of whether mineralogy plays a significant role in the protection of organic matter.

5.1. Redox conditions and organic matter preservation

Redox-sensitive trace element (RSTE) concentrations have been widely used to reconstruct palaeoredox conditions of marine sediments and sedimentary rocks, including U and Mo (Algeo and Maynard, 2004; Algeo and Lyons, 2006; Tribovillard et al., 2006; Algeo and Tribovillard, 2009; Algeo and Rowe, 2012). This research compliments other Early Palaeozoic redox studies on the Yangtze block (Wang et al., 2008; Yan et al., 2012, 2015; Zhou et al., 2015; Liu et al., 2016; Liu et al., 2018).

The lower Wufeng Formation (Stage I) displayed oxic environments in both Jiaoye 41-5 and 51-2 (Figs. 3 and 4), with moderate levels of enrichment due to partial oxidation. In contrast, the upper Wufeng Formation (Stage II in both sections; Figs. 3 and 4) exhibited higher U/Th values. Both Jiaoye 41-5 and 51-2, in terms of Mo_{EF}/U_{EF} (at the boundary of the 1× seawater curve), exhibited gradual enrichments in the Wufeng Formation, confirming anoxic-euxinic environments (Fig. 6). The OSB (Stage III) displayed a sudden environmental change in terms of the U/Th proxy, indicating high oxygen levels (Figs. 3 and 4) due to a rapid sea-level fall attributed to the Hirnantian glaciations (Zhao et al., 2017; Chen et al., 2004, 2006).

With respect to the U/Th proxy, the lower Longmaxi Formation (Stage IV) initially displayed an anoxic environment with a gradual change to sub-oxic, whereas the upper Longmaxi (Stage V) demonstrated an oxygen-rich environment. Moreover, Mo_{EF}/U_{EF} scatter plots of the Longmaxi Formation in Jiaoye 41-5 and 51-2 exhibit enrichment, indicating harsh sub-oxic or even anoxic environments (Fig. 6). The prominent anoxia in the lower Longmaxi favours organic matter preservation, which coincides with Mo_{EF}/U_{EF} values for redox conditions.

Redox proxies Mo_{EF}/U_{EF} (Fig. 6) and U/Th profiles (Figs. 3 and 4) suggest that anoxic palaeoenvironmental conditions were widespread during siliceous shale deposition, especially in the upper Wufeng and the lower Longmaxi formations, which was conducive to organic matter preservation. Towards the end of Stage IV, enhanced oxygen content (sub-oxic palaeoenvironment) is apparent, but the low concentration of dissolved oxygen in the weakly reducing sub-oxic environment was not sufficient to deteriorate the strong OCAR in the presence of high productivity. Subsequently, a slight decrease in TOC preservation was observed. Although previous research concluded that long-term stable anoxia existed within the Yangtze Sea following the Hirnantian glaciation (Chen et al., 2004; Yan et al., 2012; Zhou et al., 2015), the U/Th proxy within this study indicated fluctuating redox conditions during deposition of the lower to upper Longmaxi Formation. The upper Longmaxi (Middle Rhuddanian) experienced a new glacial epoch with a relative drop in sea level (Liu et al., 2016). Consequently, Stage V exhibited low U/Th values, indicating a gradual increase in oxygen levels that induced a strong oxic environment, resulting in low TOC values.

5.2. Role of palaeoproductivity in organic matter enrichment

Both Jiaoye 41-5 and 51-2 were divided into 5 stages on the basis of

TOC content (Figs. 3 and 4). Although no single proxy is inherently more reliable than others, palaeoproductivity assessments should generally be made on the basis of multiple proxies (Averyt and Paytan, 2004). In Jiaoye 41-5, Stage II displayed high palaeoproductivity coinciding with high values of TOC enrichment, OCAR and Bio-SiAR (Fig. 3). Stage III showed lower values for palaeoproductivity indicators, which increased sharply after the OSB. Jiaoye 51-2 (Stage II) displayed elevated values for all palaeoproductivity proxies in the upper Wufeng Formation (Fig. 4).

The lower Longmaxi Formation (Stage IV) in both Jiaoye 41-5 and 51-2 (Figs. 3 and 4) displayed good productivity indicators, validating that accumulation of the organic-rich interval in the Upper Yangtze Platform was associated with increased surface productivity. During the depositional period of the late Katian (Wufeng Stage II) and Rhuddanian (Longmaxi Stage IV), the sea level rose, leading to higher palaeoproductivity (i.e., abundant algae, graptolites and other planktonic organisms), instigating a strong reducing environment (Yan et al., 2015; C. Wu et al., 2017, J. Wu et al., 2017; Liu et al., 2017). Additionally, high organic productivity increased the flux of organic matter to the sea floor, which eventually led to organic matter enrichment, a key factor for the formation of source rocks (Pedersen and Calvert, 1990; Jin, 2001; Zhang et al., 2005). Due to sea-level fall in the upper Longmaxi Formation (Stage V), a slight decrease in productivity indicators was observed together with higher sedimentation rates (Table 2), which could have escalated the dilution of organic matter accumulation (Li et al., 2017). Consequently, an anoxic and deep siliceous-continental shelf environment developed, resulting in the formation of organic-rich siliceous, carbonaceous and siliceous-carbonaceous shales.

Stages II and IV (upper Wufeng and lower Longmaxi formations) are characterized by high organic matter abundance in both Jiaoye 41-5 and 51-2 (TOC 4–7%) and high values of OCAR, Bio-SiAR and palaeoproductivity indicators, resulting in highly favourable conditions for shale gas exploration. This observation is supported by higher Bio-Si, Cu, Ni, Ba/Al and P/Al values in the upper Wufeng and lower Longmaxi formations in these stages than in Stages I, III and V (organic-poor intervals characterized by low TOC and decreased levels of palaeoproductivity proxies). Accordingly, it was observed that the Bio-Si content of organic-rich shales was significantly better than that of organic-poor shales, showing high values in Stages II and IV from both Jiaoye 41-5 (Fig. 3) and Jiaoye 51-2 (Fig. 4), coinciding with siliceous organism abundance and organic carbon enrichment in the Wufeng and Longmaxi formations. Furthermore, the synchronous relationship between OCAR and Bio-SiAR in the studied sections, i.e., higher values in Stages II and IV than in Stages I, III and V, reinforces the fact that Bio-Si plays an important role in organic matter enrichment within marine environments.

Many researchers have performed comprehensive studies on palaeoproductivity (Tenger et al., 2006; Yan et al., 2015; Zhou et al., 2015) and the palaeoenvironment of the Wufeng-Longmaxi succession (Wang et al., 2008; Yan et al., 2015; Zhou et al., 2015; Liu et al., 2016; Luo et al., 2016), yet this study is the first to postulate how Bio-Si is directly linked to TOC in the studied palaeomarine environments.

5.3. Radiolarians, TOC and marine siliceous source rocks

Radiolarians and other siliceous organisms extract silica from seawater to form their tests, which eventually sink into sediments and are easily dissolved and recycled (Conley and Malone, 1992; Ragueneau et al., 1996; Heinze et al., 2003). The bulk of TOC in marine sediments is commonly derived from marine phytoplankton, and the results of a large number of ocean surveys show that levels of silica content and primary productivity in marine environments have good correspondence (Nelson et al., 1995; Yang et al., 2006). An abundance of radiolarians is linked with algae proliferation, and consequently, high productivity leads to an adequate supply of organic matter, providing materials that guarantee the development and deposition of high-quality siliceous source rocks (Pedersen and Calvert, 1990; Lu et al., 2018).

A large number of studies in China and abroad clearly illustrate that most marine source rocks contain silica and abundant radiolarian fossils (De Wever and Baudin, 1996; Shen et al., 2012; Cardott, 2013; Xiang et al., 2013; Shi et al., 2016; Shaldybin et al., 2017). Radiolarian blooms could lead to organic matter enrichment, resulting in the formation of high-quality source rocks (Erbacher and Thurow, 1997; Xiang et al., 2013). Globally, most siliceous formations are radiolarites, which are excellent hydrocarbon source rocks. For example, the Devonian Domanik layer in Russia is composed of radiolarian-rich siliceous mudstone (Ormistron, 1993; Vishnevskaya, 1998; Afanasieva, 2000), and the black flint series of siliceous shale in Europe are major source rocks (De Wever et al., 2001). In Northwest China, large numbers of giant oil fields located in the Tarim Basin are composed of organic-rich sedimentary strata of siliceous rocks containing radiolarians (Sun et al., 2003). Additionally, the Ediacaran Doushantuo Formation, the lower Cambrian Niutitang Formation (Zhang et al., 2007), the middle Permian Gufeng Formation and the upper Permian Dalong Formation are all marine source rocks rich in radiolarian fossils (Xia et al., 2010) with proven excellent hydrocarbon generation (Hu et al., 2004; Lv et al., 2004; Liu, 2005; Wang et al., 2006).

The direct relationship of radiolarians and sponge spicules with TOC was studied in Jiaoye 41-5, where radiolarians exhibited a low positive correlation ($R = +0.23$, $p(\alpha) > 0.05$, $n = 69$) and sponge spicules displayed a negative correlation ($R = -0.16$, $p(\alpha) > 0.05$, $n = 49$) (Fig. 7). The average abundance of radiolarians was 89 individuals/g, and that of sponge spicules was 8 individuals/g (Fig. 3), providing a ratio of 11:1, which coincides with a better correlation of TOC to radiolarians than to sponge spicules (Fig. 7).

In Jiaoye 51-2, there were no well-preserved radiolarians and very low numbers of sponge spicules; therefore, no meaningful comparisons could be made. Several factors can control the degree of preservation of siliceous organisms, including the robustness of skeletons, depositional/burial conditions and digenesis, which can lead to the dissolution or pyritization of siliceous tests.

In Mesozoic-Cenozoic marine source rocks, organic matter was mainly derived from dinoflagellates, yet for Palaeozoic marine source rocks, organic matter was generally derived from acritarchs (Du et al., 2012) (Fig. 8). However, the development of acritarchs mimics the diversity of radiolarians and giant oil fields through geological time, instigating the hypothesis that organic matter in Palaeozoic marine source rocks could have originated from radiolarians that flourished in the Early Palaeozoic (associated with high primary productivity). Although the correlation coefficient result is not statistically significant, the relative abundance results and past studies discussed above indicate that radiolarians were better contributors to TOC than sponge spicules in Jiaoye 41-5.

5.4. Bio-Si and TOC

The graptolitic-bearing black shale intervals of the Ordovician-Silurian transition in South China contain exclusively Type-I kerogen (Liu, 2005; Su et al., 2007; Tenger and Zheng, 2008; C. Wu et al., 2017, J. Wu et al., 2017), proving that aquatic organisms were the main primary producers of organic matter during the deposition of oil shale (Zou et al., 2010; Song et al., 2016). Currently, the general consensus is that phytoplankton (containing high lipid content) are the main source of hydrocarbons (Hedges and Parker, 1976; Showers and Angle, 1986; Gordon and Goni, 2004; Shen et al., 2015), whereas zooplankton are mainly composed of protein material and contribute significantly less to oil and gas accumulation. This research utilizes elemental proxies, micro-siliceous organism quantification and thin-section analysis to confirm that silica within our study area generally has a biogenic origin formed by biological sedimentation originating from Bio-Si dissolution

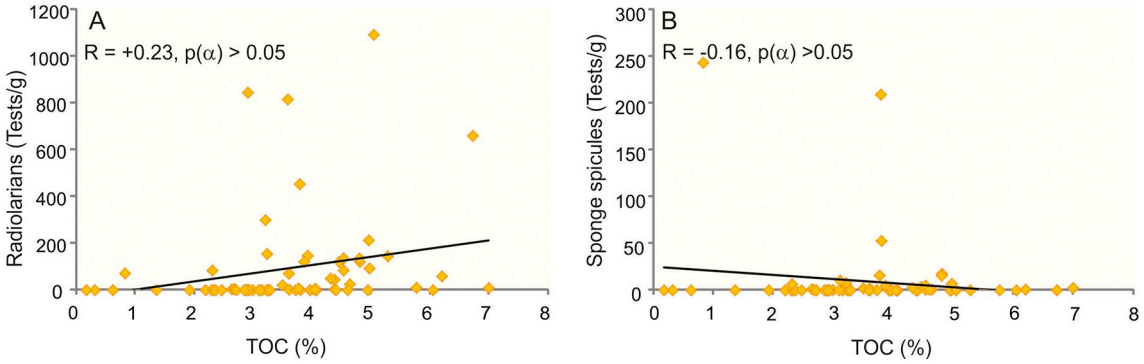

Fig. 7. Plot of micro-siliceous organism abundance versus TOC for Jiaoye 41-5. (A) Radiolarians versus TOC. (B) Sponge spicules versus TOC.

and re-crystallization of radiolarian tests and sponge spicules.

TOC is the direct record of organic carbon in sediments from oceanic surface waters, although high levels of degradation could occur during the depositional and burial processes (Tyson, 2005; Schoepfer et al., 2015). Although a weak correlation was found between radiolarians and TOC (see 5.3), a strong positive correlation was discovered between Bio-Si and TOC in the Wufeng-Longmaxi formations, specifically Jiaoye 41-5 ($R = +0.68$, $p(\alpha) < 0.01$, $n = 69$) and Jiaoye 51-2 ($R = +0.68$, $p(\alpha) < 0.01$, $n = 48$) (Fig. 9). Bio-Si, which is a strong productivity indicator for radiolarians and sponge spicules, coincides with other palaeoproductivity indicators and TOC (showing synchronous patterns for phytoplankton and micro-siliceous organisms in the studied sections), suggesting a potential mutual contribution from radiolarians to organic matter accumulation in the Wufeng and Longmaxi formations. This study provides strong evidence that certain zooplankton (in this case radiolarians) contribute significantly more towards organic matter accumulation than previously perceived, both directly and indirectly.

Thus, two plausible explanations are presented to decipher the link amongst Bio-Si, TOC and radiolarians:

(i) It is widely accepted that diatoms are the main contributors of TOC in Cenozoic source rocks, typically containing 8–40% lipids (Du et al., 2012). Likewise, studies on the chemical composition of modern radiolarians have shown that lipid contents can reach 47% (Anderson, 1983; De Wever et al., 2001; Du et al., 2012).

The average lipid content of a colony of *Collozum longiforme* is approximately 100 μg, and the total organic matter is approximately 250 μg (Anderson, 1983), conveying up to 1 g/m^3 of radiolarian lipids and 2.5 g/m^3 of radiolarian organic matter to surface waters. These colonies can attain 3 m in length with a single 50 cm long colony contributing as much primary production as 12–67 L of seawater from the oligotrophic Sargasso Sea in the equatorial Atlantic Ocean (Swanberg and Harbison, 1980). When considering the vertical flux of carbon to the sea bed, one can calculate that up to 20,000 radiolarians/m^2/day may be deposited in bottom sediments in regions such as the modern tropical Atlantic, i.e., 30 g lipid/m^2/day with 160 g OM/m^2/day. A gross estimation based on Anderson's data (Anderson, 1983) reveals that radiolarian lipids in bottom sediments may represent 15 to 50% of the total organic matter.

(ii) Radiolarians can co-exist with large numbers of microalgae (predominantly dinoflagellates), with microalgal productivity reaching up to three times that of the phytoplankton around the radiolarians (Du et al., 2012). Modern radiolarians use a large number of pseudopodia to absorb many symbiotic algae. The pseudopodial net produced by these species can be extensive and is used to ensnare and phagocytose a wide variety of prey, ranging from bacteria to relatively large zooplankton (Dennett et al., 2002), which contribute significantly to the nutrition of the host (Caron et al., 1995). Although radiolarians are capable of existing as a single cell, numerous species (largely within the order Spumellaria) form colonies of individuals by extending their cytoplasm to

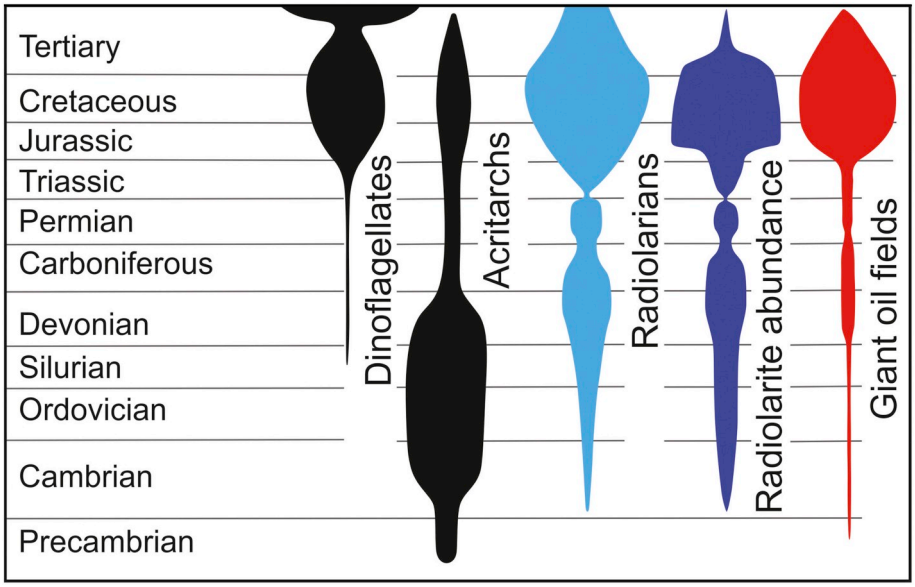

Fig. 8. Contrasts amongst radiolarian diversity, radiolarites and giant oil fields through the geological timescale (modified from Brasier, 1980; De Wever et al., 2001; Du et al., 2012).

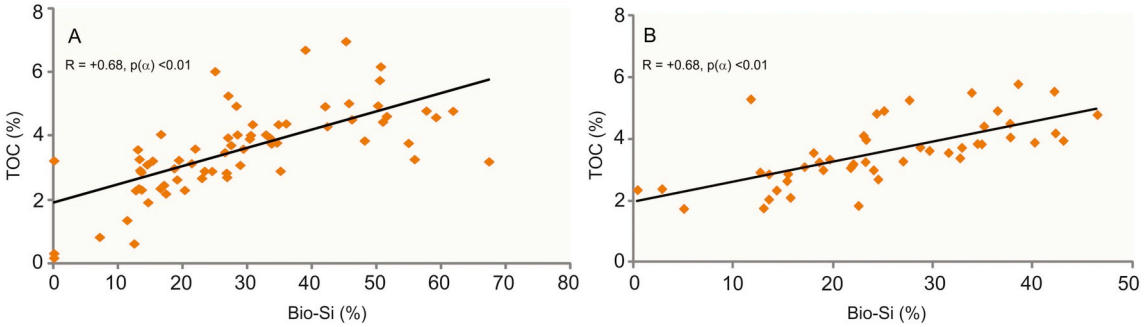

Fig. 9. Plot of Bio-Si versus TOC for the Wufeng and Longmaxi black shales of the Yangtze Platform. (A) Jiaoye 41-5 and (B) Jiaoye 51-2.

create an anastomosing web of pseudopodia enclosed within a common gelatinous matrix (Swanberg and Harbison, 1980; Du et al., 2012).

This symbiotic relationship between phytoplankton (algae) and zooplankton (radiolarians) creates two favourable factors for organic matter accumulation upon completion of the radiolarian lifecycle: (a) the intricate siliceous tests of radiolarians along with their symbiotic algae are preserved in sediments, leading to organic matter enrichment (Lu et al., 2018), and (b) symbiotic algae contained within the gelatinous matrix of radiolarian colonies can attain higher sink rates due to their denser state, leading to lower degradation through the water column. The decomposition of organic matter in the process of settlement is consequently reduced, resulting in enhanced preservation within sediments.

Subsequently, it can be concluded that radiolarians with high lipid content can contribute to not only TOC but also hydrocarbon-generating parent material by means of their habitat and symbiotic relationships with phytoplankton, in conjunction with Bio-Si occulation (intricate micro-siliceous tests), which boost organic matter accumulation.

6. Conclusions

This research demonstrated a strong direct link between Bio-Si and TOC, specifically Jiaoye 41-5 ($R = +0.68$, $p(\alpha) < 0.01$, $n = 69$) and Jiaoye 51-2 ($R = +0.68$, $p(\alpha) < 0.01$, $n = 48$), in the Wufeng-Longmaxi succession. The biogenic origin of the silica within our studied sections was established, indicating that siliceous rocks were derived from radiolarian tests and sponge spicules rather than from hydrothermal activity or a detrital origin.

The accumulation and preservation of organic matter was controlled in the entire studied section by fluctuating palaeoredox conditions, palaeoproductivity, Bio-SiAR and OCAR. The Wufeng-Longmaxi succession was divided into five stages based on organic-rich and organic-poor intervals. Stages I, III and V revealed reduced organic carbon and Bio-Si accumulation rates, with low palaeoproductivity indicators and oxygen-induced palaeomarine environments.

Stage II of the upper Wufeng Formation displayed high TOC enrichment due to extreme anoxic conditions and excellent palaeoproductivity with moderate levels of OCAR and Bio-SiAR. However, Stage IV of the lower Longmaxi Formation, despite exhibiting higher palaeoproductivity and stabilized OCAR and Bio-SiAR levels, acquired slightly lower TOC enrichment (in comparison with Stage II) due to a prevailing sub-oxic environment. Synchronous profiles of Bio-SiAR and OCAR in both Stage II of the upper Wufeng Formation and Stage IV of the lower Longmaxi Formation indicate the strong effect of marine siliceous organisms on organic carbon enrichment.

In palaeomarine environments, the study of micro-siliceous organism abundance is difficult due to ubiquitous diagenesis and dissolution phenomena. To supplement this research, several past studies based on abundant radiolarian fossils linked with siliceous source rocks worldwide were reviewed, as well as those on modern radiolarians linked with organic matter preservation.

Utilizing all aspects of this research, it can be confidently stated that Bio-Si is a major indicator for organic carbon enrichment, even in the absence of well-preserved micro-siliceous organism tests. Moreover, it is conceivable that radiolarians could have contributed unconventionally to TOC enrichment in the Wufeng-Longmaxi Palaeozoic marine source rocks, along with traditional contributors such as phytoplankton.

Acknowledgements

The author would like to thank Lei Zhang and Associate Professor Jun Shen for providing helpful insights towards the research and Hidayat-Ullah Khan for proofreading assistance. A special thanks is given to Editor-in-chief Thomas J. Algeo for detailed feedback and direction for the betterment of this manuscript. This work was supported by the State Special Fund from the Ministry of Science and Technology (2017ZX05036002 and 2016ZX05060) and the MOST State Key Laboratory of Geological Processes and Mineral Resources, China University of Geosciences in Wuhan (MSFGPMR201702).

References

Adachi, M., Yamamoto, K., Sugisaki, R., 1986. Hydrothermal chert and associated siliceous rocks from the northern Pacific their geological significance as indication of ocean ridge activity. Sediment. Geol. 47, 125–148. https://doi.org/10.1016/0037-0738(86)90075-8.

Afanasieva, M.S., 2000. Atlas of Paleozoic Radiolaria of the Russian Platform. Nauchnyi Mir, Moscow 477 (in Russian).

Algeo, T.J., Lyons, T.W., 2006. Mo-total organic carbon covariation in modern anoxic marine environments: implications for analysis of paleoredox and paleohydrographic conditions. Paleoceanography 21, PA1016. DOI: https://doi.org/10.1029/2004PA001112.

Algeo, T.J., Maynard, J.B., 2004. Trace-element behaviour and redox facies in core shales of Upper Pennsylvanian Kansas-type cyclothems. Chem. Geol. 206, 289–318. https://doi.org/10.1016/j.chemgeo.2003.12.009.

Algeo, T.J., Rowe, H., 2012. Paleoceanographic applications of trace-metal concentration data. Chem. Geol. 324, 6-18. https://doi.org/10.1016/j.chemgeo.2011.09.002.

Algeo, T.J., Tribovillard, N., 2009. Environmental analysis of paleoceanographic systems based on molybdenum–uranium covariation. Chem. Geol. 268, 211–225. https://doi.org/10.1016/j.chemgeo.2009.09.001.

Algeo, T.J., Henderson, C.M., Tong, J., Feng, Q., Yin, H., Tyson, R.V., 2013. Plankton and productivity during the permian–triassic boundary crisis: an analysis of organic carbon fluxes. Glob. Planet. Chang. 105, 52–67. https://doi.org/10.1016/j.gloplacha.2012.02.008.

Algeo, T.J., Marenco, P.J., Saltzman, M.R., 2016. Co-evolution of oceans, climate, and the biosphere during the 'Ordovician Revolution': A review. Palaeogeogr. Palaeoclimatol. Palaeoecol. 458, 1–11.

Anderson, O.R., 1983. The trophic role of planktonic foraminifera and radiolarian. Marine Microbial Food Webs 7, 31–51.

Arsairai, B., Wannakomol, A., Feng, Q., Chonglakmani, C., June 2016. 2016. Paleoproductivity and Paleoredox Condition of the Huai Hin Lat Formation in Northeastern Thailand. J. Earth Sci. 27 (3), 350–364.

Averyt, K.B., Paytan, A., 2004. A comparison of multiple proxies for export production in the equatorial Pacific. Paleoceanography 19, PA4003 (14). DOI: https://doi.org/10.1029/2004PA001005.

Bishop, J.K.B., 1988. The barite-opal-organic carbon association in oceanic particulate matter. Nature 332, 341–343.

Boström, K., Kraemer, T., Gartner, S., 1973. Provenance and accumulation rates of opaline silica, Al, Ti, Fe, Mn, Cu, Ni and Co in Pacific pelagic sediments. Chem. Geol. 11,

123–148. https://doi.org/10.1016/0009-2541(73)90049-1.
Brasier, M.D., 1980. Microfossils. George Allen and Unwin, London, pp. 21–88.
Calvert, S.E., Pedersen, T.F., 1993. Geochemistry of recent oxic and anoxic marine sediments: Implications for the geological record. Mar. Geol. 113 (1/2), 67–88.
Cardott, B., 2013. Woodford Shale: from hydrocarbon source rock to reservoir. Search and Discovery 50817, 85.
Caron, D.A., Michaels, A.F., Swanberg, N.R., 1995. Primary productivity by symbiont-bearing planktonic sarcodines (Acantharia, Radiolaria, Foraminifera) in surface waters near Bermuda. J. Plankton Res. 17, 103–129. https://doi.org/10.1093/plankt/17.1.103.
Chalmers, G., Bustin, M., Power, I., 2012. Characterization of gas shale pore systems by porosimetry, pycnometry, surface area, and field mission scanning electron microscopy/transmission electron microscopy image analyses: examples from the Barnett, Woodford, Haynesville, Marcellus, and Doig units. AAPG Bull. 96, 1099–1119. https://doi.org/10.1306/10171111052.
Chen, X., Rong, J., Li, Y., Boucot, A.J., 2004. Facies patterns and geography of the Yangtze region, South China, through the Ordovician and Silurian transition. Palaeogeogr. Palaeoclimatol. Palaeoecol. 204, 353–372. https://doi.org/10.1016/S0031-0182(03)00736-3.
Chen, X., Rong, J., Fan, J., Zhan, R., Charles, E., Mitchell, Harper D.A., Melchin, M.J., Peng, P., Finney, S.C., Wang, X., 2006. The Global Boundary Stratotype Section and Point (GSSP) for the base of the Hirnantian Stage (the uppermost of the Ordovician System). Geological Episodes (English edition) 29 (3), 183–196.
Chen, X., Zhang, Y.D., Fan, J.X., 2012. Onset of the Kwangsian Orogeny as evidenced by biofacies and lithofacies. Science China Journal of Earth Sciences 55, 1592–1600. https://doi.org/10.1007/s11430-012-4490-4.
Chen, X., Fan, J.X., Chen, Q., Tang, L., Hou, X.D., 2014. Toward a stepwise Kwangsian Orogeny. Journal of China Earth Science 57, 379–387. https://doi.org/10.1007/s11430-013-4815-y.
Chen, X., Fan, J.X., Zhang, Y.D., Wang, H.Y., Chen, Q., Wang, W.H., Liang, F., Guo, W., Zhao, Q., Nie, H.K., Wen, Z.D., Sun, Z.Y., 2015. Subdivision and delineation of the Wufeng and Longmaxi black shales in the subsurface areas of the Yangtze platform. J. Stratigr. 39, 351–358 (in Chinese with English abstract).
Chou, Y., Lou, J., Chen, C., Liu, L., 2012. Spatial distribution of sponge spicules in sediments around Taiwan and the Sunda Shelf. J. Oceanogr. 68, 905–912. https://doi.org/10.1007/s10872-012-0143-7.
Conley, D.J., Malone, T.C., 1992. Annual cycle of dissolved silicate in Chesapeake Bay: implications for the production and fate of phytoplankton biomass. Mar. Ecol. Prog. Ser. 81, 121–128. https://doi.org/10.3354/meps081121.
Dapples, C.E., 1967. Chapter 6: Silica as an agent in Diagenesis. Dev. Sedimentol. 8, 323–342.
De Wever, P., Baudin, F., 1996. Palaeogeography of radiolarite and organic-rich deposits in Mesozoic Tethys. Geol. Rundsch. 85, 310–326. https://doi.org/10.1007/BF02422237.
De Wever, P., Dumitrica, P., Caulet, J.P., Nigrini, C., Caridroit, M., 2001. Radiolarians in the sedimentary record. Gordon and Breach Science Publishers 29–76.
Dehairs, F., Stroobants, N., Goeyens, L., 1991. Suspended barite as a tracer of biogical activity in the Southern Ocean. Mar. Chem. 35, 399–410. https://doi.org/10.1016/S0304-4203(09)90032-9.
Dennett, M.R., Caron, D.A., Michaels, A.F., Gallager, M., Davis, S.C., 2002. Video plankton recorder reveals high abundances of colonial Radiolaria in surface waters of the central North Pacific. J. Plankton Res. 24, 797–805. https://doi.org/10.1093/plankt/24.8.797.
Du, Y., Jun, S., Feng, Q., 2012. Applications of radiolarians for productivity and hydrocarbon-source rock. J. Earth Sci. 37 (2), 147–155. (in Chinese with English abstract). https://doi.org/10.3799/dqkx.2012.S2.015.
Dymond, J., Suess, E., Lyle, M., 1992. Barium in deep-sea sediment: a geochemical proxy for paleoproductivity. Paleoceanography 7, 163–181. https://doi.org/10.1029/92PA00181.
Erbacher, J., Thurow, J., 1997. Influence of oceanic anoxic events on the evolution of mid-Cretaceous radiolaria in the North Atlantic and western Tethys. Marine Micropalaeontology 30, 139–158. https://doi.org/10.1016/S0377-8398(96)00023-0.
Estermann, E.F., Peterson, G.H., Mclaben, A.D., 1959. Digestion of clay-protein, lignin-protein, and silica-protein complexes by enzymes and bacteria. Soil Sci. Soc. Am. J. 23 (1), 31. https://doi.org/10.2136/sssaj1959.03615995002300010017x.
Gibbons, W., Morena, T., 2002. The geology of Spain. Gsw Books 44–45.
Gordon, E.S., Goni, M.A., 2004. Controls on the distribution and accumulation of terrigenous organic matter in sediments from the Mississippi and Atchafalaya river margin. Mar. Chem. 92 (1), 331–352. https://doi.org/10.1016/j.marchem.2004.06.035.
Gradstein, F.M., Ogg, J.G., Schmitz, M.A., Ogg, G. (Eds.), 2012. The Geologic Time Scale, Vol. 2. Elsevier, Amsterdam.
Griffith, E.M., Paytan, A., 2012. Barite in the ocean–occurrence, geochemistry and palaeoceanographic applications. Sedimentology 59, 1817–1835. https://doi.org/10.1111/j.1365-3091.2012.01327.x.
Guo, T., 2013. Evaluation of highly thermally mature shale-gas reservoirs in complex structural parts of the Sichuan Basin. J. Earth Sci. 24 (6), 863–873. https://doi.org/10.1007/s12583-013-0384-4.
Hedges, J.I., 1995. Sedimentary organic matter preservation: an assessment and speculative synthesis. Mar. Chem. 49 (2–3), 123–126. https://doi.org/10.1016/0304-4203(95)00008-F.
Hedges, J.I., Parker, P.L., 1976. Land-derived organic matter in surface sediments from the Gulf of Mexico. Geochimimica et Cosmochimica Acta 40, 1019–1029. https://doi.org/10.1016/0016-7037(76)90044-2.
Heinze, C., Hupe, A., Maier-Reimer, E., 2003. Sensitivity of the marine biospheric Si cycle for biogeochemical parameter variations. Glob. Biogeochem. Cycles 17, 12–18. https://doi.org/10.1029/2002GB001943.
Hu, W., Lv, B., Shen, W., 2004. Characteristics of upwelling sedimentation in Cambrian in Southeast Margin of Yangtze Plate. Journal of Petroleum Institute 26 (4), 9–11 (in Chinese with English abstract).
Huerta-Diaz, M.A., Morse, J.W., 1992. Pyritisation of trace metals in anoxic marine sediments. Geochim. Cosmochim. Acta 56, 2681–2702. https://doi.org/10.1016/0016-7037(92)90353-K.
Ingall, E., Bustin, R.M., Van Cappellen, P., 1993. Influence of water column anoxia on the burial and preservation of carbon and phosphorus in marine shales. Geochim. Cosmochim. Acta 57, 303–316. https://doi.org/10.1016/0016-7037(93)90433-W.
Ingri, J., Widerlund, A., Suteerasak, T., Bauer, S., Åke Elming, A., 2014. Changes in trace metal sedimentation during freshening of a coastal basin. Mar. Chem. 167, 2–12. https://doi.org/10.1016/j.marchem.2014.06.010.
Jin, Q., 2001. The importance of effective hydrocarbon source rock and its research. Oil and gas geology and harvesting rate 8 (1), 1–5 (in Chinese with English abstract).
Keil, R.G., Mayer, L.M., 2014. Mineral matrices and organic matter. In: Treatise on Geochemistry, 2nd ed. Elsevier, pp. 337–359.
Keil, R.G., Tsamakis, E., Wolf, N., Hedges, J.I., GonÄi, M,A., 1997. Relationships between organic carbon preservation and mineral surface area in Amazon Fan sediments (Sites 932A and 942A). In Proceedings of ODP, Scientific Results, Vol. vol. 155, ed. R. D. Flood, D. J. W. Piper, A. Klaus and L. C. Peterson. Ocean Drilling Program, College Station, TX.
Lazarus, D., 1994. An improved cover-slip holder for preparing microslides of randomly distributed particles. J. Sediment. Res. 64 (3a), 686. https://doi.org/10.2110/jsr.64.686.
Lewan, M.D., Maynard, J.B., 1982. Factors controlling enrichment of vanadium and nickel in the bitumen of organic sedimentary rocks. Geochimimica et Cosmochimica Acta 46 (12), 2547–2560. DOI: 0016-7037/82/122547-14S03.00/0.
Li, J., Xie, X.N., Lin, Z., 2009. Organic matter enrichment of the Dalong Formation in Guangyuan area of the Sichuan basin. Geological Science and Technology Information 28, 98–103 (in Chinese with English abstract).
Li, Y., Zhang, T., Ellis, G.S., Shao, D., 2017. Depositional environment and organic matter accumulation of Upper Ordovician–Lower Silurian marine shale in the Upper Yangtze Platform, South China. Palaeogeogr. Palaeoclimatol. Palaeoecol. 466, 252–264. https://doi.org/10.1016/j.palaeo.2016.11.037.
Liang, D., Guo, T., Chen, J., Bian, L., Zhao, Z., 2009. Some progresses on studies of hydrocarbon generation and accumulation in marine sedimentary region, southern China (part 2): geochemical characteristics of four suits of regional marine source rocks, South China. Marine Origin Petroleum Geology 14 (1), 1–15 (in Chinese with English abstract).
Liu, G.X., 2005. Characteristics of Middle Paleozoic marine source rock in the north margin of middle and upper Yangtze region. Petroleum Geology and Experiment 27 (5), 490–495 (in Chinese with English abstract).
Liu, Z., Algeo, T.J., Guo, X.S., Fan, J., Du, X., Lu, Y., 2016. Paleo-environmental cyclicity in the early Silurian Yangtze Sea (South China): Tectonic or glacio-eustatic control? Palaeogeogr. Palaeoclimatol. Palaeoecol. 466, 59–76. https://doi.org/10.1016/j.palaeo.2016.11.007.
Liu, J., Yao, Y., Elsworth, D., Liu, D., Yidong, C., Dong, L., 2017. Vertical heterogeneity of the shale reservoir in the lower Silurian Longmaxi Formation: analogy between the southeastern and northeastern Sichuan Basin, SW China. Minerals 151, 1–17. https://doi.org/10.3390/min7080151.
Liu, K., Feng, Q., Jun, S., Khan, M., Planavsky, N.J., 2018. Increased productivity as a primary driver of marine anoxia in the Lower Cambrian. Palaeogeogr. Palaeoclimatol. Palaeoecol. 491, 1–9. https://doi.org/10.1016/j.palaeo.2017.11.007.
Lu, L., Qin, J. Z., Shen, B.J., Tenger., Lui, W.X., Zhaang, Q.Z., 2018. Biogenetic evidence of siliceous shale in the Wufeng Formation-Longmaxi Formation in the Upper Yangtze area and its relationship with shale gas enrichment. Journal of Geoscience, 2018(4), 226–236 (in Chinese with English abstract). DOI: 10.13745/J.ESF.YX.2017-5-5
Luo, Q.Y., Zhong, N.N., Dai, N., Zhang, W., 2016. Graptolite-derived organic matter in the Wufeng-Longmaxi Formations (Upper Ordovician– lower Silurian) of Southeastern Chongqing, China: implications for gas shale evaluation. Int. J. Coal Geol. 153 (1–2), 87–98. https://doi.org/10.13039/501100001809.
Lv, B., Wang, H., Hu, W., 2004. Relationship between Paleozoic upwelling facies and hydrocarbon in southeastern marginal Yangtze Block. Marine Geology and Quaternary Geology 24(4), 29–35 (in Chinese with English abstract). DOI: 10.16562/j.cnki.0256-1492.2004.04.005
Lyle, M., Murray, D.W., Finney, B.P., 1988. The record of late Pleistocene sedimentation in the eastern tropical Pacific Ocean. Paleoceanography 3, 39–59. https://doi.org/10.1029/PA003i001p00039.
Metcalfe, I., 1994. Late Paleozoic and Mesozoic palaeogeography of eastern Pangaea and Tethys. Canada Society of Petroleum Geologists Memoir 17, 97–111.
Morse, J.W., Luther III, G.W., 1999. Chemical influences on trace metal–sulphide interactions in anoxic sediments. Geochim. Cosmochim. Acta 63, 3373–3378. https://doi.org/10.1016/S0016 -7037(99)00258-6.
Mou, C.L., Zhou, K.K., Liang W., Ge, X.Y., 2011. Early Paleozoic sedimentary environment of hydrocarbon source rocks in the Middle–Upper Yangtze Region and petroleum and gas exploration. Acta Geologica Sinica 85(4), 526–532. DOI: 11–1951/P.20110330.0842.025.
Muller, P.J., Suess, E., 1977. Interaction of organic compounds with calcium carbonate. Amino acid composition of sorbed layers. Geochim. Cosmochim. Acta 41 (7), 941–949.
Murphy, A.E., Sageman, B.B., Hollander, D.J., Lyons, T.W., Brett, C.E., 2000. Black shale deposition and faunal overturn in the devonian appalachian basin: clastic starvation, seasonal water-column mixing, and efficient biolimiting nutrient recycling.

Paleoceanography 15 (3), 280–291. https://doi.org/10.1029/1999pa000445.
Nelson, D.M., Paul, T., Brzezinski, M.A., Leynaert, A., Bernard, Q., 1995. Production and dissolution of biogenic silica in the ocean: revised global estimates, comparison with regional data and relationship to biogenic sedimentation. Glob. Biogeochem. Cycles 9(3), 359-0. DOI: https://doi.org/10.1029/95gb01070.
Nie, H., Jin, Z.J., Zhang, J.C., 2018. Characteristics of three organic matter pore types in the Wufeng-Longmaxi Shale of the Sichuan Basin. Southwest China. Scientific reports 8, 7014. https://doi.org/10.1038/s41598-018-25104-5ID.
Ormistron, A.R., 1993. The association of radiolarians with the hydrocarbon source rocks. In: Murchey, B.L. (Ed.), Blueford J.R. Micropaleontology Special Publication, Radiolaria of giant and subgiant fields in Asia, pp. 9–16.
Pedersen, T.F., Calvert, S.E., 1990. Anoxia vs. productivity: what controls the formation of organic carbon rich sediments and sedimentary rocks? AAPG Bull. 74, 454–472. https://doi.org/10.1306/0C9B232B-1710-11D7-8645000102C1865D.
Piccara, J.M., Storch, P., Gutierrez-Marco, J.C., Oliveira, J.T., 1995. Characterization of the Parakidograptus acuminatus graptolite Biozone in the Silurian of the Barrancos region. (Ossa Morena Zone, South Portugal). Communications of Geological and minning institute 81, 3–8.
Piper, D.Z., Perkins, R.B., 2004. A modern vs. Permian black shale the hydrography, primary productivity, and water-column chemistry of deposition. Chem. Geol. 206, 177–197. https://doi.org/10.1016/j.chemgeo.2003.12.006.
Porter, S.J., Selby, D., Cameron, V., 2014. Characterising the nickel isotopic composition of organic-rich marine sediments. Chem. Geol. 387, 12–21. https://doi.org/10.1016/j.chemgeo.2014.07.017.
Ragueneau, O., Leynaert, A., Tréguer, P., Demaster, D.J., Anderson, R.F., 1996. Opal studied as a marker of paleoproductivity. Eos Transactions American Geophysical Union 77 (49), 491. https://doi.org/10.1029/96EO00325.
Ran, B., Liu, S.G., Jansa, L., Sun, W., Yang, D., Ye, Y.H., Wang, S.Y., Luo, C., Zhang, X., Zhang, C.J., 2015. Origin of the Upper Ordovician–lower Silurian cherts of the Yangtze block, South China, and their palaeogeographic significance. J. Asian Earth Sci. 108, 1–17. https://doi.org/10.1016/j.jseaes.2015.04.007.
Rangin, C., Steinberg, M., Bonnot-Courtois, C., 1981. Geochemistry of the Mesozoic bedded cherts of Central Baja California (Vizcaino-Cedros-San Benito): implications for paleogeographic reconstruction of an old oceanic basin. Earth Planet. Sci. Lett. 54, 313–322. https://doi.org/10.1016/0012-821X(81)90014-5.
Redfield, A.C., 1960. The biological control of chemical factors in the environment. Sci. Program. 11 (11), 150–170.
Reolid, M., Rodriguez-Tovar, F.J., Marok, A., 2012. The Toarcian oceanic anoxic event in the Western Saharan Atlas, Algeria (North African Paleomargin): role of anoxia and productivity. Geol. Soc. Am. Bull. 124 (9/10), 1646–1664. https://doi.org/10.1130/b30585.1.
Robin, E., Rabouille, C., Martinez, G., Lefevre, I., Reyss, J., Van, B., Jeandel, C., 2003. Direct barite determination using SEM/EDS-ACC system: implication for constraining barium carriers and barite preservation in marine sediments. Mar. Chem. 82, 289–306. https://doi.org/10.1016/S0304-4203(03)00075-6.
Rona, P.A., 1988. Hydrothermal mineralization at oceanic ridges. Can. Mineral. 26, 431–465.
Ross, D., Bustin, R.M., 2009. The importance of shale composition and pore structure upon gas storage potential of shale gas reservoirs. Mar. Pet. Geol. 26, 916–927. https://doi.org/10.1016/j.marpetgeo.2008.06.004.
Ruiz-Ortiz, P.A., Bustillo, M.A., Molina, J.M., 1989. Radiolarite Sequences of the Subbetic, Betic Cordillera, Southern Spain. Siliceous Deposits of the Tethys and Pacific Regions. Springer New York, pp. 107–127. https://doi.org/10.1007/978-1-4612-3494-4_8.
Sageman, B., Murphy, A., Werne, J., Ver Straeten, C., Hollander, D., Lyons, T., 2003. A tale of shales: the relative roles of production, decomposition, and dilution in the accumulation of organic-rich strata, Middle-Upper Devonian, Appalachian basin. Chem. Geol. 195 (1), 229–273. https://doi.org/10.1016/S0009-2541(02)00397-2.
Schenau, S.J., Reichart, G.J., Lange, G.J.D., 2005. Phosphorus burial as a function of paleoproductivity and redox conditions in Arabian Sea sediments. Geochim. Cosmochim. Acta 69 (4), 919–931. https://doi.org/10.1016/j.gca.2004.05.044.
Schoepfer, S.D., Shen, J., Wei, H., Tyson, R.V., Ingall, E., Algeo, T,J., 2015. Total organic carbon, organic phosphorus, and biogenic barium fluxes as proxies for paleomarine productivity. Earth Sci. Rev. 149(2015), 23–52. DOI: https://doi.org/10.1016/j.earscirev.2014.08.017.
Sclater, F.R., Boyle, E., Edmond, J.M., 1976. On the marine geochemistry of nickel. Earth & Planetary Science Letters 31 (1), 119–128. https://doi.org/10.1016/0012-821X(76)90103-5.
Shaldybin, M.V., Lopushnyak, Y.M., Goncharov, I.V., Wilson, M.J., Wilson, L., Mendis, B.G., 2017. The mineralogy of the clayey-silty siliceous rocks in the Bazhenov Shale Formation (Upper Jurassic) in the west Siberian Basin, Russia: the role of diagenesis and possible implications for their exploitation as an unconventional hydrocarbon reservoir. Appl. Clay Sci. 136, 75–89. https://doi.org/10.1016/j.clay.2016.11.009.
Shen, J., Algeo, T.J., Hu, Q., Xu, G., Zhou, L., Feng, Q., 2012. Volcanism in South China during the Late Permian and its relationship to marine ecosystem and environmental changes. Glob. Planet. Chang. 105, 121–134. https://doi.org/10.1016/j.gloplacha.2012.02.011.
Shen, J., Lian, Z., Feng, Q.L., Zhang, M.H., Yong, L., Ning, Z., 2014. Paleoproductivity evolution across the Permian-Triassic boundary and quantitative calculation of primary productivity of black rock series from the Dalong Formation, South China. Science China Earth Sciences 57, 1583–1594. https://doi.org/10.1007/s11430-013-4780-5.
Shen, J., Schoepfer, S.D., Feng, Q., Zhou, L., Yu, J., Song, H., Wei, H., Algeo, J.T., 2015. Marine productivity changes during the End-Permian crisis and Early Triassic recovery. Earth Sci. Rev. 149, 136–162. https://doi.org/10.1016/j.earscirev.2014.11.002.
Shen, J., Algeo, T.J., Chen, J., Planasky, N.J., Feng, Q., Yu, J., Liu, J., 2019. Mercury in marine Ordovician/Silurian boundary sections of South China is sulfide-hosted and non-volcanic in origin. Earth Planet. Sci. Lett. 522, 130–140. https://doi.org/10.1016/j.epsl.2019.01.028.
Shi, L., Feng, Q., Shen, J., Ito, T., Chen, Z., 2016. Proliferation of shallow-water radiolarians coinciding with enhanced oceanic productivity in reducing conditions during the Middle Permian, South China: evidence from the Gufeng Formation of western Hubei Province. Palaeogeogr. Palaeoclimatol. Palaeoecol. 444, 1–14. https://doi.org/10.1016/j.palaeo.2015.11.031.
Showers, W.J., Angle, D.G., 1986. Stable isotopic characterization of organic carbon accumulation on the Amazon continental shelf. Continntal Shelf Research 6, 227–244. https://doi.org/10.1016/0278-4343(86)90062-2.
Song, Y., Liu, Z., Meng, Q., Xu, J., Sun, P., Cheng, L., 2016. Multiple controlling factors of the enrichment of organic matter in the upper cretaceous oil shale sequences of the songliao basin, NE China: implications from geochemical analyses. Oil Shale 33 (2), 142–166. https://doi.org/10.3176/oil.2016.2.04.
Storch, P., Kraft, P., 2009. Graptolites assemblages and stratigraphy of the lower Sulrian Mrakotin Formation, Hlinsko Zone, NE interior of the Bohemian massif (Czech Republic). Bull. Geosci. 84 (1), 51–74. https://doi.org/10.3140/bull.geosci.1077.
Su, W.B., Li, Z.M., Ettensohn, F.R., Johnson, M.E., Huff, D., Wang, W., Ma, C., Li, L., Zhang, L., Zhao, J.J., 2007. Tectonic and eustatic control on the distribution of black shale in the Wufeng– Longmaxi Formations (Ordovician-Silurian), South China: major controlling factors and implications. Frontiers of Earth Science in China 1, 470–481. https://doi.org/10.1007/s11707-007-0058-6.
Suess, E., 1973. Interaction of organic compounds with calcium carbonate. Organo-carbonate associations in recent sediments. Geochim. Cosmochim. Acta 37 (11), 2435–2447.
Sun, S.L., Chen, J.F., Liu, W.H., 2003. Hydrothermal venting on the seafloor and formation of organic-rich sediments- evidence from the Neoproterozoic Xiamaling Formation, North China. Geological Review 49(6), 588–595(in Chinese with English abstract).
Sunda, W.G., Barber, R.T., Huntsman, S.A., 1981. Phytoplankton growth in nutrient rich seawater-importance of copper-manganese cellular interactions. J. Mar. Res. 39, 567–586.
Swanberg, N.R., Harbison, G.R., 1980. The ecology of Collozoum longiforme, sp.nov. a new colonial radiolarian from the equatorial Atlantic Ocean. Deep sea Research Part A. Oceanographic research papers 27, 715–731. https://doi.org/10.1016/0198-0149(80)90024-2.
Taylor, S.R., McLennan, S.M., 1985. The Continental Crust: it's Composition and Evolution, an Examination of the Geochemical Record Preserved in Sedimentary Rocks. The Continental Crust: Its Composition and Evolution: An Examination of the Geochemical Record Preserved in Sedimentary Rocks. Blackwell Scientific Publication, Oxford, pp. 31.
Tenger, Q.J., Zheng, L., 2008. Spatiotemporal distribution of Sinian-Permian excellent marine source rocks in southeastern Guizhou province. Marine Origin Petroleum Geology 13 (2), 37–44 (In Chinese with English abstract).
Tenger, Q.J., Gao, C.L., Hu, K., Pan, W.L., Zhang, C.J., Fang, C.M., Cao, Q.G., 2006. High-quality source rocks in the lower combination in southeast Upper-Yangtze area and their hydrocarbon generating potential. Pet. Geol. Exp. 28 (4), 360–365 (in Chinese with English abstract).
Tribovillard, N., Algeo, T.J., Lyons, T., Riboulleau, A., 2006. Trace metals as paleoredox and paleoproductivity proxies: an update. Chem. Geol. 232, 12–32. https://doi.org/10.1016/j.chemgeo.2006.02.012.
Tyson, R.V., 2005. The "productivity versus preservation" controversy; cause, flaws, and resolution. In: Harris, N.B. (Ed.), Deposition of Organic-Carbon-Rich Sediments:Models Mechanisms, and Consequences: Society for Sedimentary Geology (SEPM-SSG) Special Publication. vol. 82. pp. 17–33.
Van der Weijden, C.H.V.D., 2002. Pitfalls of normalization of marine geochemical data using a common divisor. Mar. Geol. 184 (3/4), 167–187. https://doi.org/10.1016/s0025- 3227(01)00297-3.
Vishnevskaya, V.S., 1998. The domanikoid facies of the Russian platform and basin paleogeoraphy. In Carsquin-Soeau.S., Barrier, E., eds. Stratigraphy and Evolutionof Peri-Tethiyanplatforms. Memoirs Museum National Histoire Naturelle, Paris 177, 45–69.
Wang, K., Chatterton, B.D.E., Wang, Y., 1997. An organic carbon isotope record of Late Ordovician to early Silurian marine sedimentary rocks, Yangtze Sea, South China: implications for CO2 changes during the Hirnantian glaciation. Palaeogeogr. Palaeoclimatol. Palaeoecol. 132, 147–158. https://doi.org/10.1016/S0031-0182(97)00046-1.
Wang, Y.G., Wen, Y.C., Hong, H.T., Xia, M.L., Song, W., 2006. Dalong Formation found in Kaijiang-Liangping oceanic trough in Sichuan Basin. Nat. Gas Ind. 26 (9), 32–36 (in Chinese with English abstract).
Wang, Q.C., Yan, D.T., Li, S.J., 2008. Tectonic-environmental model of the lower Silurian high quality hydrocarbon source rocks from South China. Acta Geol. Sin. 82 (3), 289–297 (in Chinese with English abstract).
Wang, S., Wang, L., Huang, J., 2009. Accumulation condition of shale gas reservoirs in Silurian of the Upper Yangtze region. Nat. Gas Ind. 29 (5), 45–50.
Wang, X., Zhu, Y., Lash, G.G., Wang, Y., 2019. Multi-proxy analysis of organic matter accumulation in the Upper Ordovician-Lower Silurian black shale on the upper Yangtze Platform, South China. Mar. Pet. Geol. https://doi.org/10.1016/j.marpetgeo.2019.03.013.
Weiler, R.R., Mills, A.A., 1965. Surface properties and pore structure of marine sediments. Deep-Sea Res. 12, 511–529.
Wignall, P.B., Myers, K.J., 1988. Interpreting benthic oxygen levels in mudrocks: a new approach. Geology 16 (5), 452–455. https://doi.org/10.1130/0091-7613(1988)0162.3.CO;2.

Wu, C., Tuo, J., Zhang, M., Liu, Y., Xing, L., Gong, J., Qiu, J., 2017. Multiple controlling factors of Lower Palaeozoic organic-rich marine shales in the Sichuan Basin, China: evidence from minerals and trace elements. Energy Exploration &Exploitation 35 (5), 627–644. https://doi.org/10.1177/0144598717709667.

Wu, J., Liang, F., Lin, W., Wang, H., Bai, W.H., Ma, C., Sun, S., Zhao, Q., Song, X., Yu, R., 2017. Characteristics of shale gas reservoirs in Wufeng Formation and Longmaxi Formation in well WX2, Northeast Chongqing. Petroleum Research 2, 324–335. https://doi.org/10.1016/j.ptlrs.2017.05.002.

Xia, M.L., Wen, L., Wang, Y.G., 2010. High-quality source rocks in trough facies of the Upper Permian Dalong Formation of Sichuan basin. Petroleum Exploration Development 37, 654–662 (in Chinese with English abstract).

Xiang, Y., Feng, Q., Shen, J., Zhang, N., 2013. Changhsingian radiolarian fauna from Anshun of Guizhou, and its relationship to TOC and paleoproductivity. Science China Earth Sciences 56, 1334–1342. https://doi.org/10.1007/s11430-013-4615-4.

Yamamoto, K., 1987. Geochemical characteristics and depositional environments of cherts and associated rocks in the Franciscan and Shimanto terrenes. Sediment. Geol. 52, 65–108. https://doi.org/10.1016/0037-0738(87)90017-0.

Yan, D.T., Chen, D.Z., Wang, Q.C., Wang, J.G., 2012. Predominance of stratified anoxic Yangtze Sea interrupted by short-term oxygenation during the Ordo-Silurian transition. Chem. Geol. 291, 69–78. https://doi.org/10.1016/j.marpetgeo.2015.04.016.

Yan, D., Wang, H., Fu, Q., Chen, Z., He, J., Gao, Z., 2015. Geochemical characteristics in the Longmaxi Formation (early Silurian) of South China: Implications for organic matter accumulation. Mar. Pet. Geol. 65, 290–301. https://doi.org/10.1016/j.marpetgeo.2015.04.016.

Yang, D.F., Zhenhui, G., Yingbin, Y., Peiyan, S., Xinping, W., 2006. Silicon limitation on primary production and its destiny in Jiaozhou bay. Chinese Journal of Oceanology and imnology, 24(4), 401–412. DOI: https://doi.org/10.1007/BF02842857.

Yuan, J., Yang, J., Ma, H., Liu, C., Zhao, C., 2016. Hydrothermal synthesis of analcime and hydroxycancrinite from K-feldspar in Na_2SiO_3 solution: characterization and reaction mechanism. RSC Adv. 6, 54503–54509. https://doi.org/10.1039/C6RA08080D.

Zeng, X.L., Liu, S.G., Huang, W.M., Zhang, C.J., 2011. Comparison of Silurian Longmaxi Formation shale of Sichuan Basin in China and Carboniferous Barnett Formation shale of Fort Worth Basin in United States. Geological Bulletin of China 30 (2/3), 372–384 (in Chinese with English abstract).

Zhang, S., Zhang, B., Zeng, B., 2005. Development constraints of marine source rocks in China. Earth Science Frontiers 12 (3), 39–48 (in Chinese with English abstract).

Zhang, L.W., Huang, J.H., Liang, Q., Zhou, Y., 2007. Geological characteristics and ore prospect of the black layers in the Doushantuo and Niutitang formations in Guizhou Province. Acta Mineral. Sin. 27, 456–460 (in Chinese with English abstract).

Zhao, J., Jin, Z.K., Jin, Z., Wen, X., Geng, Y., 2017. Origin of authigenic quartz in organic-rich shales of the Wufeng and Longmaxi Formations in the Sichuan Basin, South China: Implications for pore evolution. Journal of Natural Gas Science and Engineering 38, 21–38. https://doi.org/10.1016/j.jngse.2016.11.037.

Zhou, L., Algeo, T.J., Shen, J., Hu, Z.F., Gong, H.M., Xie, S.C., Huang, J.H., Gao, S., 2015. Changes in marine productivity and redox conditions during the Late Ordovician Hirnantian glaciation. Palaeogeogr. Palaeoclimatol. Palaeoecol. 420, 223–234.

Zou, C., Dong, D., Wang, S., Li, J., Li, X., Wang, Y., Li, D., Cheng, K., 2010. Geological characteristics and resource potential of shale gas in China. Pet. Explor. Dev. 37, 641–653. https://doi.org/10.1016/S1876-3804(11)60001-3.